ELSEVIER

Contents lists available at ScienceDirect

# **Energy & Buildings**

journal homepage: www.elsevier.com/locate/enb



# Direct heat flux sensing for window shading control in passive cooling systems



Jackson Danis <sup>a</sup>, Sandipan Mishra <sup>b</sup>, Alexandra R. Rempel <sup>c,\*</sup>

- <sup>a</sup> Thayer School of Engineering, Dartmouth College, Hanover, NH 03755, United States
- <sup>b</sup> Department of Mechanical, Aerospace, and Nuclear Engineering, Rensselaer Polytechnic Institute, Troy, NY 12180, United States
- <sup>c</sup> Environmental Studies Program, University of Oregon, Eugene, OR 97403, United States

#### ARTICLE INFO

#### Article history: Received 30 October 2021 Revised 5 January 2022 Accepted 10 February 2022 Available online 22 February 2022

Keywords: Climate-responsive control Infinite impulse response filter Endpoint moving average filter Arduino EnergyPlus Co-simulation

#### ABSTRACT

Greenhouse gas emissions from space cooling are expected to double globally by 2050, giving urgency to the development of low-carbon cooling methods. Solar heat gain through windows is a leading contributor to cooling loads, and accordingly, operable shading strategies have been established that respond to numerous environmental parameters, including solar radiation, illumination, time of day, and indoor and outdoor air temperature. While these have shown excellent performance, optimal setpoints are typically specific to climates, seasons, and spaces, preventing development of controls with consistent effectiveness across varying conditions. Here we investigate an alternative parameter, window surface heat flux, in which a universal setpoint of 0W/m² identifies transitions between window heat gain and loss. Examination of heat flux signals acquired with low-cost sensors first revealed the associated noise to be consistent but too great for control application. Representative noise characteristics were then used to construct noisy signals for simulations, allowing evaluation of noise mitigation by digital filtering methods and signal persistence requirements. Strikingly, shading controlled by the resulting output reduced window heat gain by 54–78% in six contrasting climates, comparable to or exceeding the performance of established approaches, indicating that heat flux sensing is now an outstanding candidate for shading control in passive cooling systems.

© 2022 Elsevier B.V. All rights reserved.

# 1. Introduction

Space cooling is the most rapidly growing energy use in buildings worldwide, expected to triple by 2050 to a level exceeding 6000 TWh annually. Greenhouse gas emissions are projected double accordingly, reflecting partial decarbonization of the world's electrical systems but nevertheless exceeding 2000 MMT per year [1], creating an urgent need for non-mechanical space cooling strategies [2]. Even in the U.S., where per-capita use is greatest, air conditioning is expanding rapidly: currently consuming 4% of all U.S. energy, and emitting nearly 150 MMT of CO<sub>2</sub> each year, U. S. space cooling energy use is expected to grow by over 50% by 2050 [3,4]. The result is renewed interest in passive cooling systems such as window shading, night ventilation of mass, radiative cooling, and passive evaporative cooling, as well as passive-active hybrids such as evaporative coolers and fan-assisted night ventilation, reviewed recently in [5].

Solar heat gain through unshaded windows is a prominent contributor to space-cooling loads in both residential and nonresidential buildings [e.g. 6,7], particularly in those with high window-to-wall ratios and single glazing [e.g. 8,9]. In buildings with windows oriented toward the equator or the direction of sunset, solar heat gain has the potential to drive peak cooling loads as well [e.g. 10]. Building energy efficiency codes limit window solar heat gain in warmer climates by requiring glazing with low solar heat gain coefficients (SHGC), but they allow higher values in cooler climates where solar energy is needed to offset heating loads [11,12]. As a result, effective shading is a valuable method of limiting window heat gain and diminishing cooling loads even in cool climates [13]. This importance has given rise to widespread interest in the effectiveness of operable shading devices and associated control strategies. It is now well-known that shading device performance is improved by exterior positioning, for example, allowing the device to intercept solar radiation before it enters the building [e.g. 14,15]. When interior shading is necessary, performance is improved by high material reflectance; low visible and solar transmittance; and the sealing of shade edges to prevent room air from circulating between the shade and the window

<sup>\*</sup> Corresponding author.

E-mail address: arempel@uoregon.edu (A.R. Rempel).

Nomenclature					
EMA IIR $\phi$ S $F$ $\Delta$ $N$ $\alpha$ $n$ $T_{sol}$	Endpoint moving average filter Infinite impulse response filter Noise-free (true) heat flux signal (W/m²) Noisy heat flux signal (W/m²) Filtered heat flux signal (W/m²) Random variable used in noise models EMA interval (timesteps) IIR coefficient (dimensionless) Measurement index (current timestep) Transmitted solar radiation (W/m²)	$I_{sol}$ $\sigma$ $\mu$ $P$ $ACH_{50}$ $U$ $T_{vis}$ $R_{vis}$ SHGC	Incident solar radiation (W/m²) Standard deviation Mean Persistence interval (timesteps) Air changes per hour under 50 Pa Thermal transmittance (W/m²K) Visible transmittance (fraction) Visible reflectance (fraction) Solar heat gain coefficient (fraction)		

[16–18]. Additionally, shade retraction allows windows to radiate energy to cooler outdoor surroundings at night, as shown by [16,19] and evidence below.

Shading control has been studied primarily in the context of highly glazed and dynamic facades in office buildings, in which cooling considerations are often integrated with those of daylighting and visual comfort [e.g. 10,20-23]. Since photosensors are inexpensive and widely used in electric light-dimming applications, illumination has become a popular environmental parameter for shading control in multiple forms, including workplane illuminance [22], transmitted illuminance [21], beam illuminance on window surfaces [10], and exterior illuminance [24]. Workplane illuminance recommendations have ranged from minima of 100-600 lux to maxima of 1280-1800 lux [20]; similarly, transmitted illuminance recommendations have ranged from 9000-45,000 lux [21], reflecting the diversity of spaces, seasons, and climates studied, and highlighting the often space-specific nature of illumination setpoints. Still, when space-specific optimization is possible, and especially when electric lighting is simultaneously dimmed in response to daylight availability, shading controlled to maintain illumination within specified bounds can reduce annual cooling (as well as lighting) loads considerably [e.g. 10].

Shading control for glare reduction is also well-studied in workspaces, in which blinds are raised or lowered, or blind slats are tilted, such that the Daylight Glare Index (DGI) at specified positions in the space remains below specified setpoints, typically 22-24 [20,25,26]. Since blinds controlled in this way preferentially intercept beam solar radiation through windows, which contributes directly to cooling loads, glare control has reduced cooling loads by 15–22% in some studies [25,20]. It has had weaker effects in other studies [26], however, suggesting that this visual metric, like illuminance, may have idiosyncratic cooling effects. Studies focused on cooling load reduction therefore often employ measures more closely related to solar radiation intensity at window surfaces, such as the quantity incident upon an exterior window surface,  $I_{sol}$ , or the quantity transmitted through the window,  $T_{sol}$ . These parameters are directly related to window heat gain, giving them advantages over illumination measurements alone when cooling load reduction is a priority. Accordingly, shading controlled by these parameters has reduced cooling loads and/or overheated hours substantially, with values of approximately 60% reported in multiple studies [7,20,27]. The primary disadvantage of solar radiation-based shading control, however, is the expense of the pyranometers required for its measurement (approx.\$300 USD or more; e.g. Apogee SP-214-SS), especially for residential applications. Additionally, ideal  $I_{sol}$  and  $T_{sol}$  setpoint values are, like those of illuminance, characteristic of individual spaces:  $T_{sol}$  and  $I_{sol}$  values studied have each ranged over an order of magnitude or more (20-400 W/m<sup>2</sup> and 50-500 W/m<sup>2</sup>, respectively), with recommended values interspersed throughout [7,20,21,27,28].

To supplement solar radiation measurements for cooling purposes, some studies have incorporated indoor air or operative temperature setpoints into shading control algorithms [7,19,27]. These allow shading to be delayed until cooling loads are present, particularly in offices, and they have addressed cooling loads quite effectively: reductions of approximately 50% or more have been accomplished in Minneapolis MN, Washington D.C., and Atlanta GA, for example [19]. Finally, shading controls have been reduced to time-of-day schedules for residential applications, consistent with time-of-day patterns observed in typical manual operation. While simple and imprecise, these have nevertheless proven effective as well, reducing cooling loads by about 20% in the climates studied [29,30].

Although the studies above are focused on lighting and visual comfort, they reveal several important themes with respect to cooling, which is the focus of the current effort. First, shading has shown the ability to reduce cooling loads consistently and appreciably across climates and occupancy types. Second, the cooling effectiveness of shading is dramatically improved by operational strategies that respond to indoor and outdoor environmental conditions. When well-suited to the space, these strategies not only diminish window solar heat gain but limit increases in heating and lighting loads that can result from excessive shading. Third, the environmental parameters most widely used in shading control schemes tend to require space-specific setpoints (e.g. illuminance) and/or expensive instruments (e.g. pyranometers), while parameters such as air temperature and time of day are less effective. Finally, signaled control of shading is far less studied in residences than in offices, despite the fact that residential buildings account for the majority of the cooling demand worldwide [1] and that cooling needs are of greater priority than lighting needs in areas that are unoccupied during daytime hours, as many resi-

The problem that remains is therefore the development of a shade control parameter with a consistent setpoint across spaces, seasons, and climates that is sufficiently affordable for residential use. To address this problem, here we investigate a promising alternative to illuminance and solar radiation sensing: the direct measurement of heat flux at window interior surfaces. Heat flux sensors are thermopile devices that generate electrical voltage signals proportional to heat exchange rates through their surfaces; the heat flux through the sensor (W/m<sup>2</sup>) is then calculated from the voltage according to the sensor's calibration properties. Heat flux sensing has numerous applications in earth, soil, and building sciences [31–33], and though heat flux sensing has primarily been used in building applications to evaluate thermal transmittance (U-) values of opaque walls, [e.g. 34], it is also well-established in window solar heat gain research [35]. A primary advantage of heat flux sensing for shading control is the existence of a universal setpoint, 0W/m<sup>2</sup>, with which to signal operation: when heat flux to

the interior is positive and cooling is desired, shades should be activated; when the heat flux direction is reversed, as occurs on summer nights in many climates, shades should be retracted. The main obstacles to the use of heat flux sensors for this purpose, in turn, include high noise levels in their measurements [31,36], physical fragility, and cost (approx.\$300 USD or more; e.g. Omega HFS-5). The emergence of more durable and lower-cost sensors, however (approx.\$50; e.g. FluxTeq PHFS-01), has addressed the latter two problems, leaving noise as the central issue to be resolved.

The purpose of the present study is to evaluate the ability of direct heat flux measurements, with noise mitigation and algorithmic interpretation, to provide effective signals for the control of operable window shades for cooling. Using a combination of field measurements, digital filtering, signal persistence requirements, and MATLAB-EnergyPlus co-simulations, we investigate the ability of heat flux-based signals to reduce window solar heat gain across hot desert, cold semi-arid, humid subtropical, humid continental. and Mediterranean climates in residential spaces. We find that shading in response to appropriately filtered and interpreted heat flux signals reduces window solar heat gain to equal or greater extents than illumination- and incident solar radiation-based controls in each climate, revealing heat flux to be a highly effective, widely applicable parameter with which to signal shade operation for cooling. These results further suggest that heat flux sensing has the potential to replace solar radiation measurements in applications that integrate cooling load reductions with lighting and visual comfort criteria.

## 2. Methods

The work below combines physical data collection and simulation. Physical data were acquired to facilitate the characterization of real noise in heat flux measurements, as well as to allow the creation of realistic synthetic noise; simulations, in turn, were conducted to understand the effects of noise in heat flux signals on shading performance.

#### 2.1. Field investigation

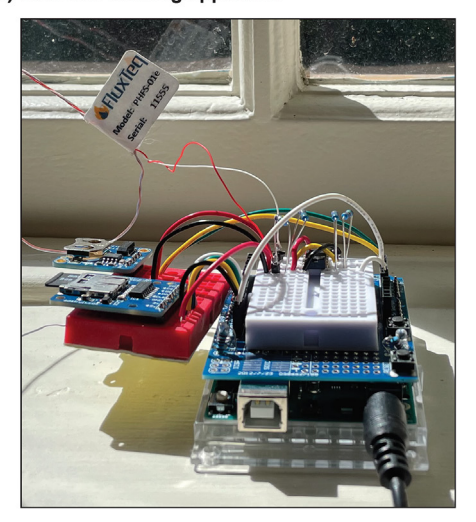
#### 2.1.1. Heat flux measurements

To collect heat flux measurements for noise characterization and modeling, FluxTeq (www.fluxteq.com) PHFS-01e thermopile heat flux sensors (sensitivity:  $1.06\pm0.03 \,\mu\text{V}/(\text{W/m}^2)$ ; range: ±150 kW/m<sup>2</sup>) were applied to the interior surfaces of doubleglazed east-, south-, and west-facing windows at the University of Oregon in Eugene OR. These heat flux signals were transmitted to Arduino Uno R3 boards, amplified by two-stage OPA2336P operational amplifiers (Mouser Electronics; www.mouser.com) with negative feedback to control gain (Fig. 1), and recorded on microSD cards using Adafruit (www.adafruit.com) ADA254 breakout boards. Adafruit DS 1307 Real Time Clocks were used, in addition, to improve the timing accuracy of Arduino microprocessors. Measurements were recorded at 30s intervals unless otherwise specified. Because heat flux values recorded on west windows were affected by thermal fluctuations (i.e. wind, partial tree shading, occupancy, equipment, and fans) to a greater extent than those collected from east and south windows, the noise characteristics of west window heat flux measurements were used for all subsequent analyses, including co-simulations.

# 2.1.2. Signal characterization

To search for repeating artifacts and unexpected (i.e. non-diurnal) periodicity in heat flux signals, we performed both a fast Fourier transform, examining periods as brief as one minute in length, and an autocorrelation analysis, examining time lags at

#### a) Heat flux sensing apparatus



#### b) Amplification circuit

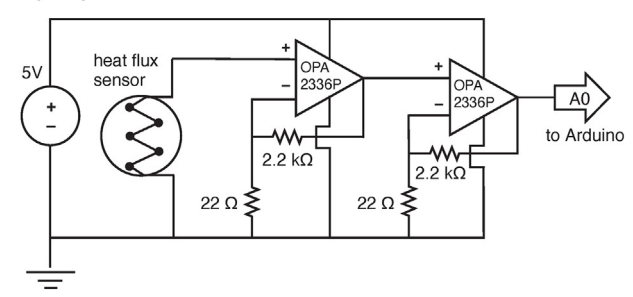


**Fig. 1.** Heat flux sensing and amplification apparatus. Heat flux measurements were a) recorded using FluxTeq PHFS-01e thermopile heat flux sensors with Arduino Uno R3 boards and b) amplified with two-stage OPA2336P operational amplifiers with negative feedback.

intervals of 30s from 0 to 33.3h, on measurements collected from the west-facing window over the five days of July 8–12, 2021, inclusive.

#### 2.2. Building energy performance simulations

#### 2.2.1. EnergyPlus modeling

All simulations were conducted in EnergyPlus 9.2, a researchgrade building energy modeling tool [37], using weather files representing typical conditions over the years of 2004–2018 [38] (see also Section 2.2.2). These investigations employed a one-bedroom multifamily dwelling based on the design of Seattle architecture firm Mithun, Inc. (https://mithun.com/), with south-facing orientation and with envelope assemblies compliant with climatespecific requirements of the 2018 International Energy Conservation Code (IECC), including vertical glazing area of less than 15% of the conditioned floor area [11]. Glazing assemblies were created in WINDOW 7.7 [39] and imported into EnergyPlus as spectral IDF objects, representing code minimum values in each climate; opaque envelope components and envelope air leakage (infiltration) properties were those required in colder climates throughout, exceeding requirements in warmer climates (Table 2). For simplicity, internal heat gain rates, including contributions from occupancy, lighting, and equipment, were held constant at the level prescribed by the 2018 IECC [11]. Geometry was specified in Euclid 0.9.4.2 [40], an open-source extension for SketchUp (www. sketchup.com), and materials, internal heat gains, ventilation, and infiltration were specified directly in the EnergyPlus IDF editor. Maximum indoor temperatures were limited to 25°C (77°F) by

Ideal Loads Air System objects, and all simulations were conducted with timesteps of 1 min.

#### 2.2.2. Climate and interval selection

A central motivation for the study of heat flux sensing is the potential applicability of a single threshold, 0W/m<sup>2</sup>, to varying climatic conditions for effective shading control. To investigate this potential, and to compare it to the analogous capacity of established shading control parameters and thresholds, we selected six distinct climates, including hot desert, cold semi-arid, humid subtropical, warm-summer Mediterranean, hot-summer humid continental, and warm-summer continental (Table 1) to represent typical ranges of summer outdoor air temperatures, global horizontal radiation levels, and sun angles across the continental U.S. Within this group, Seattle WA was chosen to represent Pacific Northwest conditions, rather than Eugene OR where physical studies were conducted, because of its greater recognizability to international readers. To illustrate details of shading control performance, Denver CO was chosen as the representative city because of its mid-latitude position within the group, and the three-day period of July 16-18 was chosen as an interval suitable for visualizing control behavior near the peak of each city's cooling season. Summaries of the corresponding results are provided for all six cities in each case.

#### 2.2.3. Shading control

Interior shading was defined by Window Shading Control objects to specify insulated cellular shades, edge-sealed by side and bottom channels (Table 2). Shading control was accomplished through the EnergyPlus External Interface using the MATLAB-EnergyPlus Co-Simulation Toolbox [43] according to the strategies shown in Table 3. Shading activation thresholds for established parameters were adopted from investigations of setpoints for illumination [e.g. 21], incident solar radiation [e.g. 27], and high outdoor air temperature and/or high glare [e.g. 26,44,7], here represented by hours of the day. The illumination setpoint of 5000 lux, at a position immediately (20 cm) inside the window, was chosen to represent interior workplane illuminance values of 600–2,000 lux [21]; window surface heat flux, in turn, responded to the EnergyPlus output variable Surface Window Net Heat Transfer Rate. Whereas established shading control parameters are known to require climate-, season-, and even space-specific

**Table 1**Climates and weather files.

City	Köppen climate <sup>1</sup>	IECC climate <sup>2</sup>	Weather file <sup>3</sup>
Phoenix AZ	BWh: hot desert	2B	USA_AZ_Phoenix-Sky.Harbor. Intl.AP.722780_TMYx.2004- 2018.epw
Atlanta GA	Cfa: humid subtropical	3A	USA_GA_Atlanta-Hartsfield- Jackson.Intl. AP.722190_TMYx.2004–2018. epw
Seattle WA	Csb: warm- summer Mediterranean	4C	USA_WA_Seattle-Tacoma.Intl. AP.727930_TMYx.2004-2018. epw
Chicago IL	Dfa: hot- summer humid continental	5A	USA_IL_Chicago.OHare.Intl. AP.725300_TMYx.2004-2018. epw
Denver CO	BSk: cold semi- arid	5B	USA_CO_Broomfield-Rocky. Mountain.Metro. AP.724699_TMYx.2004–2018. epw
Burlington VT	Dfb: warm- summer humid continental	6A	USA_VT_Burlington.Intl. AP.726170_TMYx.2004-2018. epw

<sup>&</sup>lt;sup>1</sup>[41,42], <sup>2</sup>[11], <sup>3</sup>[38].

**Table 2**Model parameters.

viodei parameters.					
Element	Properties <sup>1</sup>				
Multifamily dwelling					
Floor area	44.9 m <sup>2</sup> (483 ft <sup>2</sup> )				
Exterior façade area	20.5 m <sup>2</sup> (221 ft <sup>2</sup> )				
Window to wall ratio	24.7% (building); 7% (dwelling)				
Exterior façade orientation	South				
Location	Top floor				
Glazing properties					
Area	Large bedroom window: 0.93 m <sup>2</sup> (10 ft <sup>2</sup> ) Total: 5.1 m <sup>2</sup> (54.5 ft <sup>2</sup> )				
U-value	IECC climates 2–4B: 1.79 W/m <sup>2</sup> K (0.32 Btu/h ft <sup>2</sup> °F)				
	IECC climates 4C–6: 1.61 W/m <sup>2</sup> K (0.28 Btu/h ft <sup>2</sup> °F)				
Solar heat gain coefficient	IECC climates 2–4B: 0.26				
	IECC climates 4C-6: 0.55				
Shading					
Optical properties	$T_{vis}$ =0.1; $R_{vis}$ =0.8				
Thermal properties	$U = 2.8 \text{ W/m}^2\text{K} (0.5 \text{ Btu/h ft}^2 ^{\circ}\text{F, or 'R-2'})$				
Edge conditions	Track-sealed (opening multipliers = 0)				
Roof assembly					
U-value	0.15 W/m <sup>2</sup> K (0.026 Btu/h ft <sup>2</sup> °F)				
Solar reflectance	0.3				
Heat capacity	310 kJ/m <sup>3</sup> K				
Exterior wall assembly					
U-value	0.32 W/m <sup>2</sup> K (0.057 Btu/h ft <sup>2</sup> °F)				
Solar reflectance	0.3				
Heat capacity	390 kJ/m <sup>3</sup> K				
Interior wall assembly					
U-value	Adiabatic (interior)				
Heat capacity	140 kJ/m <sup>3</sup> K				
Floor assembly					
U-value	Adiabatic (interior)				
Heat capacity	2010 kJ/m³K				
Internal heat gain	8.6 W/m <sup>2</sup> (0.8 W/ft <sup>2</sup> )				
Air exchange	2, 22,				
Ventilation for fresh air	0.007 m <sup>3</sup> /s (15 ft <sup>3</sup> /min)				
Air leakage	3 <i>ACH</i> <sub>50</sub>				

<sup>&</sup>lt;sup>1</sup>Thermal and optical properties reflect the requirements of the 2018 International Energy Conservation Code for residential buildings [11].

**Table 3** Shading control strategies.

Environmental parameter	Shading control
None (negative baseline)	NS: No shading
None (positive baseline)	FS: Full continuous shading
None (random operation)	RS: Shading status chosen randomly at each 1 min timestep
Time <sup>1</sup>	TD: Shading active mid-day (10a-4p)
	TA: Shading active afternoon and evening (2p-8p)
Incident solar radiation $(I_{sol})^2$	IS1: Shading active if $I_{sol} > 250 \text{ W/m}^2$
	IS2: Shading active if $I_{sol} > 50 \text{ W/m}^2$
Illumination adjacent to the window <sup>3</sup>	IL: Shading active if illumination >5000 lux; once active, retracted only if illumination < 500 lux
Interior surface heat flux $(\phi)^4$	HF: Shading active if $\phi > 0$ W/m <sup>2</sup>
Interior surface heat flux with persistence	HF-P: Shading active if $\phi>0$ W/m²; once active, retracted only if $\phi\leqslant0$ W/m² for 40 min continuously

<sup>1</sup>Derived from investigations of shade deployment under conditions of high outdoor air temperature and/or high glare [26,44,7], here converted to hours of the day for consistency among climates. <sup>2</sup>Adopted from the investigations of [27], using the EnergyPlus variable Surface Outside Face Incident Solar Radiation Rate per Area. <sup>3</sup>Adopted from the investigations of [21], corresponding to interior workplane illuminance values of approx.600-2,000 lux. <sup>4</sup>Quantified by the EnergyPlus variable Surface Window Net Heat Transfer Rate.

setpoints for effective operation [e.g. 21,27], the intriguing promise of heat flux as a control parameter lies in the potential for a single setpoint,  $0W/m^2$ , to be used across all climates, avoiding the need to determine unique values for each individual circumstance. To reveal the extent of this potential, in comparison with those of established parameters, identical setpoints were used for each shading strategy across all climate types.

#### 2.2.4. Noise simulation

Shading control by noisy heat flux signals was simulated in EnergyPlus with the assistance of the MATLAB-EnergyPlus Co-Simulation Toolbox [43]. At each 1-min timestep, window surface heat flux values were first calculated by EnergyPlus using solar radiation values from the corresponding weather files; these values were then transmitted to MATLAB and modified according to one of the noise models below (Section 2.3). Digital filters were applied, where specified, to reduce the noise. Shading responses to the resulting signals were then determined (detailed below; Section 2.3.4) and transmitted to EnergyPlus, providing the corresponding shade operation and allowing calculation of window surface heat flux values in the next timestep.

#### 2.3. Noise models

To understand the effects of noise in heat flux sensor measurements on shading control, as well as the ability of digital filtering to diminish these effects, we simulated shading performance with EnergyPlus models in which either realistic or synthetic noise was injected into the noise-free heat flux values generated by simulations.

#### 2.3.1. Realistic noise

To represent realistic noise in heat flux measurements, we collected 12 datasets, each of 2 min duration, on multiple days in July and August, 2021. Each of these recorded heat flux at intervals of 126±1.8 ms, where uncertainty in collection intervals resulted from jitter in Arduino processing times. Mean signal values remained constant over these short sampling periods, as confirmed by linear regression (slope < 0.001 W/m<sup>2</sup> in each case). Two contrasting datasets were then selected to represent high signal levels, typical of mid-day and afternoon values (median = 86.3; mean = 90.6;  $\sigma$ =28.1 W/m<sup>2</sup>), and low signal levels, typical of early morning and evening values (median = 5.4, mean = 5.3,  $\sigma$ =0.2 W/ m<sup>2</sup>), respectively. The mean value of each set was then subtracted from each constituent data point, yielding two vectors of residuals. Random sampling of the vector derived from high heat flux values created realistic noise for addition to positive heat flux values acquired from EnergyPlus simulation output, while sampling of the vector derived from low heat flux values created realistic noise for addition to non-positive values.

#### 2.3.2. Synthetic noise

To examine the effects of a range of noise magnitudes on shading performance, including levels both greater and less than those observed in physical heat flux data, we also created signals with synthetic noise. These simulated both additive noise, to model many common noise types, and multiplicative noise to mimic the presence of increasing Johnson-Nyquist noise [45,46] in the thermopiles as window surface temperatures rose throughout each day. To construct signals with additive noise, we approximated the measured noise distributions by sampling a random variable  $\Delta$  from a Gaussian probability density function with  $\mu_{\Delta}=0$  and prescribed standard deviation  $\sigma_{\Delta} \in [0,500]$  with increments of 25 W/m². This random variable was added to noise-free, simulated heat flux signals  $\phi$  as shown in Eqn.1 to create noisy signals S:

$$S = \phi + \Delta. \tag{1}$$

To generate synthetic signals S with multiplicative noise, each noise-free signal  $\phi$  was multiplied by a random variable  $(1+\Delta)$ , sampled from a Gaussian probability density function with  $\mu_{(1+\Delta)}=1$  and prescribed standard deviation  $\sigma_{(1+\Delta)}$ , as shown in Eqn. 2:

$$S = \phi(1 + \Delta). \tag{2}$$

In this case, standard deviations were chosen from

$$\sigma_{(1+\Delta)} \in \{0, \ 0.1, \ 0.2, \ 0.3, \ 0.4, \ 0.5, \ 0.7, \ 1, \ 1.5, \ 2, \ 3, \ 4, \ 5, \\ 6, \ 7, \ 8, \ 9, \ 10\}$$

#### 2.3.3. Bias

To examine the effects of negative bias (i.e. underestimation of magnitude) in heat flux signals on shading performance, we next subtracted values ranging from 0–40 W/m² from clean signals at each timestep. This bias range encompassed all values observed in physical measurements and extended to nearly ten times their magnitude. Positive bias values (representing signal overestimation) were not examined, since their effects are easily eliminated by raising the threshold for shade operation to match the observed bias value.

# 2.3.4. Digital filtering and signal interpretation

Noisy signals were filtered, where indicated, by either endpoint moving average (EMA) or infinite impulse response (IIR) filters. EMA filters replaced each heat flux value with the mean of the previous *N* measurements (Eqn. 3):

$$F_n = \frac{1}{N} \sum_{n=N+1}^{n} S_k, \tag{3}$$

where N = 20 unless otherwise specified based on the optimum found in a parametric search over values of 0–60 (Fig.S1, Supplementary Information). IIR filters, in turn, replaced each heat flux value with a weighted sum of the current measurement and the previous filtered value (Eqn. 4):

$$F_n = \alpha F_{n-1} + (1 - \alpha)S_n, \tag{4}$$

where the previous filtered value was initialized at  $0W/m^2$ . In all results shown,  $\alpha$ =0.95, the optimal value found in a parametric search over the range of 0 to 1 (Supplementary Information, Fig. S1), removing fluctuations of higher frequency than 20 min. Additionally, requirements for signal persistence were imposed where indicated, either alone or in combination with one of the filters above:

$$\{F_{n-P},\ldots,F_n\} \leq 0$$
, retract shade, else, activate shade; (5)

where P = 40 was found to be optimal (Fig. S1).

# 2.4. Study limitations

The field component of this work examined measurements provided by a single heat flux sensor model, the FluxTeq PHFS01-e, and a single microprocessor apparatus and amplification circuit (Section 2.1). The characterization of realistic noise is therefore potentially unique to the studied system, although similar noise has been reported elsewhere [e.g. 31,36]. To compensate for this limitation, we expanded the investigation of noise consequences for shading control to levels beyond those observed by creating signals with synthetic noise (Section 2.3). A second, related limitation is that the method described requires sufficient knowledge of sensor noise characteristics to determine the IIR filter coefficient α

and the EMA interval N. Likewise, knowledge of the signal bias is required to distinguish positive from negative values accurately. Third, the glazing types used in the simulations represent climate-specific 2018 International Energy Conservation Code requirements (Table 2), causing window solar heat gain coefficients (SHGC) to represent those of double glazed, low-emissivity assemblies. Windows with higher SHGC values would benefit to greater extents from shading, for cooling purposes, but would allow greater quantities of heat to enter than shown in the results below; windows with lower SHGC, in turn, would benefit to lesser extents from shading, though shading is considered valuable in reducing solar heat gain even through triple glazed windows [e.g. 47,48]. Fourth, the focus of this study is on the relative performance of shading controlled by window surface heat flux under varying levels of noise, alongside that of established shading control strategies: this work does not attempt to find optimal timepoints for shading operation, nor to find deviations of control actions from these optima. Finally, this study investigates shading control for cooling applications exclusively; optimization of shading control in response to potentially competing goals of visual comfort, daylighting, and cooling is beyond the present scope. At the same time, this work creates a foundation for the incorporation of heat flux sensing into future investigations of more complex systems.

#### 3. Results and discussion

#### 3.1. Potential effectiveness of heat flux in shading control

To understand the potential ability of heat flux signals to control shading effectively for cooling, compared to the abilities of established parameters and setpoints, we first simulated the performance of established control strategies adopted from [27,21,20,7,26,44] to that of heat flux control with a setpoint of 0W/m<sup>2</sup> (Table 3), distinguishing net window heat gain (i.e. positive heat flux) from heat loss, in a south-facing dwelling in the semiarid climate of Denver, CO (Table 1). Without shading, net window heat gain showed the expected pattern of daytime peaks, reaching approximately 165W, followed by appreciable heat loss at night with maximum rates of approximately -16W (Fig. 2a). Continuous application of interior insulated edge-sealed shading, in turn, illustrated the maximum daytime effectiveness, in which peak heat gain rates were diminished to approximately 50W. Continuous shading also revealed the penalty of nighttime shade deployment, in which desirable heat loss was approximately halved (Fig. 2b).

The addition of afternoon and evening shading (2p-8p), representing shade activation during the warmest hours of the day with retraction near sunset, diminished window heat gain when shading was active but began too late in the day to reduce total values substantially (Fig. 2c). A related strategy, in which shading was deployed during the middle of the day, diminished total heat gain to a much greater extent but was still activated too late and retracted too early to provide the maximum cooling benefit possible (Fig. 2d). Interior illumination was next investigated due to its popularity in non-residential shading control [e.g. 22,23], although illumination values depend on interior reflectance, distance from windows, and other factors, causing setpoints to be spacespecific [e.g. 21]. As expected, therefore, the illumination threshold of 5000 lux, at a position 20 cm interior to the window, offered little cooling improvement over timed controls (Fig. 2e). It is nevertheless possible that space- and season-specific illumination thresholds could be tailored to cooling; they would simply require adjustment as the relationship of illumination to net window heat gain changed throughout the year. Solar radiation incident on exterior window surfaces,  $I_{sol}$ , and transmitted solar radiation,  $T_{sol}$ , considered next, are frequently used for shading control for cooling purposes in simulation studies [e.g. 10,27,28], in which they are often highly effective because they are directly proportional to window heat gain. Consistent with such results, shading activated above the relatively low incident solar radiation threshold of  $50 \text{ W/m}^2$  reduced window heat gain extensively, diminishing it to nearly the greatest extent possible with the interior shade provided (Fig. 2f). This parameter therefore set a performance standard for heat flux control, although its field measurement is more expensive. Use of a higher  $I_{sol}$  threshold,  $250 \text{ W/m}^2$ , allowed window heat gain to increase accordingly (Fig. 2g).

Shading control in response to heat flux through window surfaces, in contrast to the strategies above, has been largely overlooked. Still, this metric could plausibly serve as an excellent signal for cooling purposes because it measures window heat gain more directly than  $I_{sol}$  or  $T_{sol}$ , allowing it to identify the transitions between window heat gain and loss that indicate the need for shading deployment or retraction more consistently. Comparisons of coincident values of window surface heat flux, interior illumination close to the window surface, and incident and transmitted solar radiation illustrate this point in the Supplementary Information: over the months of July and August in semi-arid Denver, window surface heat flux values of 0 W/m<sup>2</sup>, marking transitions between net window heat gain and loss, coincided with incident solar radiation values ranging from 0–50 W/m<sup>2</sup>; transmitted solar radiation values of 0-20W/m<sup>2</sup>, and illumination values of 0-2000 lux (Fig. S2). These ranges expanded when additional months and cities were considered (Fig.S3). Consistent with these observations, shading deployment when window heat flux to the interior was positive (Fig. 2h) accomplished daytime cooling as extensive as that observed with continuous shading (Fig. 2b), while nighttime heat loss was as extensive as that of windows without shading (Fig. 2a), improving upon the performance of control based on Isol. In other words, simulated heat flux-based control allowed shading operation to coincide closely with transitions between window heat gain and window heat loss, providing the greatest possible cooling with the equipment provided.

To our knowledge, however, only two studies have investigated window shading or movable insulation control in response to surface heat flux [44,49], and while these showed promising results, neither addressed the complications involved in direct field measurements. One explanation may be that, until recently, even the least-expensive heat flux sensors have sold for \$300 (USD) or more (e.g., Omega HFS-5). Additionally, heat flux sensors typically deliver output in microvolts, requiring amplification; the output is typically noisy [e.g. 36,50]; sensor wiring connections are often fragile; and no interface linking heat flux readings to visual signals or actuation devices appears to be commercially available. Further, and perhaps for these reasons, building energy simulation tools typically do not include window heat flux alongside illumination, incident solar radiation, indoor air temperature, and other builtin shading control parameters [e.g. 37]. Now, however, lowercost and more durable sensors have been developed, including the model used here, that invite further investigation.

Examination of the shading strategies above, again assuming noise-free signals, revealed similar resultsin the climates of Phoenix AZ, Denver CO, Atlanta GA, Seattle WA, Chicago IL, and Burlington VT (Fig. 3): the greatest reductions in window heat gain, compared to unshaded conditions, were accomplished by shading control in response to  $I_{sol}$  with a low setpoint of  $50 \text{W/m}^2$  (IS2), reducing window heat gain by 44-76%, and by interior surface heat flux with a setpoint of  $0 \text{W/m}^2$  (HF), reducing window heat gain by 54-78%. Afternoon shading (TA) was consistently ineffective, as observed in Fig. 2c, while controls based on illumination (IL) and high  $I_{sol}$  of  $250 \text{W/m}^2$  (IS1) showed mixed performance among the climates.

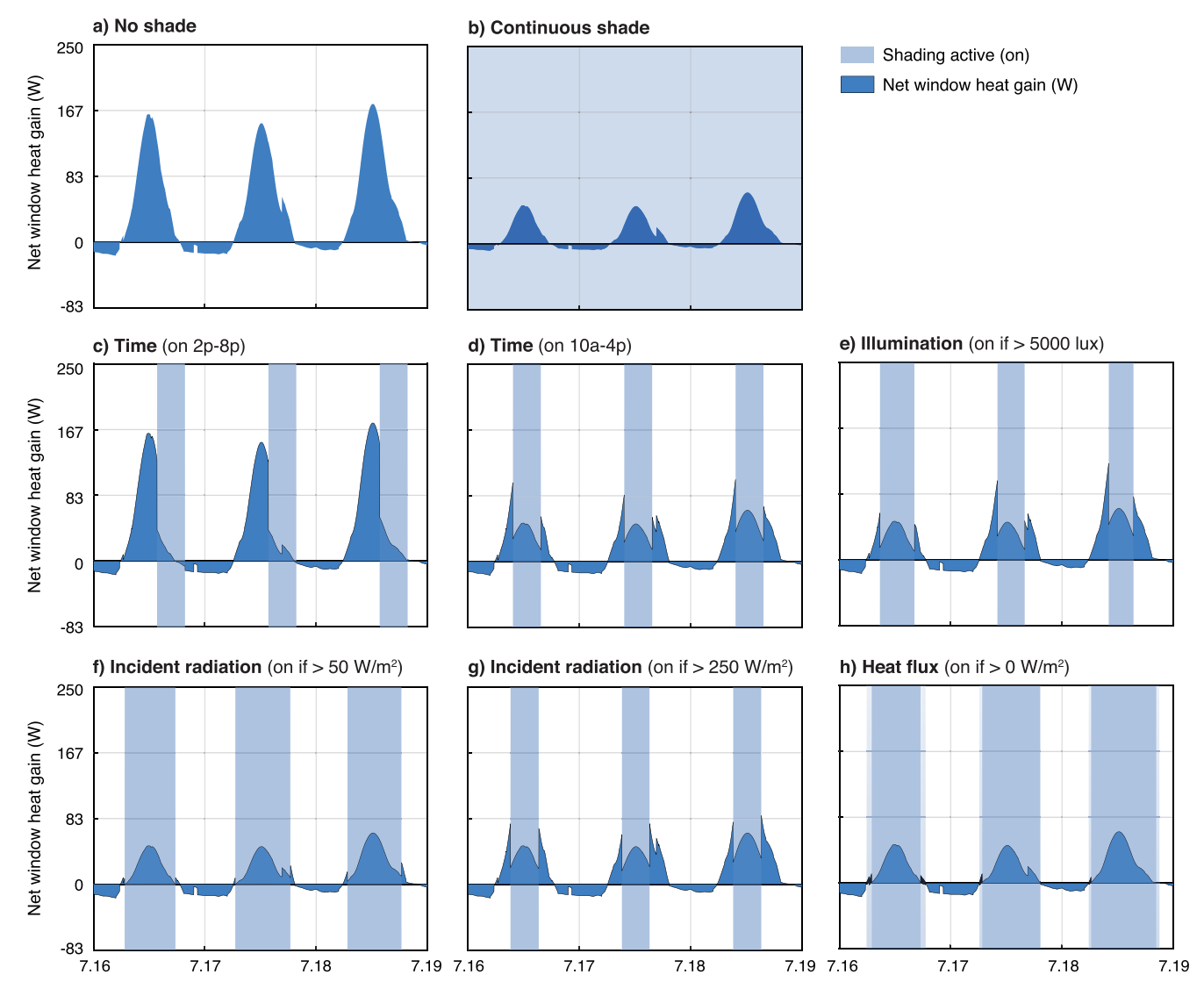


**Fig. 2.** Shading effectiveness under established and heat flux-based control strategies. Net heat gain through individual south-facing windows  $(0.93 \text{ m}^2; \text{Table 2})$  is shown at 1 min timesteps, both a) in the absence of shades and b-h) with insulating, edge-sealed shades controlled according to the following parameters: b) active continuously; c) active from 2p-8p, representing use during typically warm hours of the day; d) active from 10a-4p, representing use during hours of typically high solar radiation; e) active when interior illumination 20 cm inside the window exceeds 5000 lux, and retracted when illumination falls below 500 lux; f) active when exterior incident solar radiation exceeds  $50 \text{W/m}^2$ ; g) active when incident solar radiation exceeds  $250 \text{W/m}^2$ ; and h) active when heat flux into the dwelling is greater than  $0 \text{W/m}^2$ . Simulations represent July 16-18 performance under 2004-2018 weather typical of Denver, CO (Table 1; [38]).

#### 3.2. Heat flux measurements

To understand the feasibility of using low-cost heat flux sensors for shading control in built systems, we first collected heat flux measurements from sensors installed on east-, south-, and westfacing window interior surfaces at the University of Oregon in Eugene. Measurements from the west window, recorded at 30s intervals, showed a consistent pattern over five consecutive days in which periods of high heat flux to the interior regularly occurred mid-afternoon, before the window was shaded by an adjacent building (Fig. 4a). Noise levels were substantial during periods of positive (inward) heat flux ( $\mu$ =0.2W/m<sup>2</sup>;  $\sigma$ =32.0W/m<sup>2</sup>). During periods of zero or negative (i.e., outward) heat flux, however, readings showed little variation due to the inability of the Arduino apparatus to read negative voltages through its analog pins [51]. As a result, the system recorded all negative heat flux values as zero, obscuring most signal fluctuation when the window was losing heat. The signal feature of greatest importance for shading control in cooling applications, however, is not the magnitude of individual measurements but the clarity and accuracy of the transition between window heat loss and gain. Throughout our field measurements, exemplified by those of July 10, 2021 (Fig. 4b), these transitions were characterized by the appearance of positive noise either tens of minutes in advance of a rising baseline, as inward heat flux began, or by the comparable lingering of positive noise after the signal baseline had reached zero. These characteristics confirmed that signal noise would require mitigation and that the effectiveness of mitigation strategies would require evaluation through their impacts on shading performance.

#### 3.3. Noise characterization

To inform the development of effective noise mitigation strategies, we next examined the heat flux measurements for periodicity and distribution consistency. First, to reveal the presence of regularly repeating artifacts, a fast Fourier transform was performed on the July 8–13, 2021 dataset shown in Fig. 4a. This confirmed that diurnal fluctuations were the greatest oscillations present,

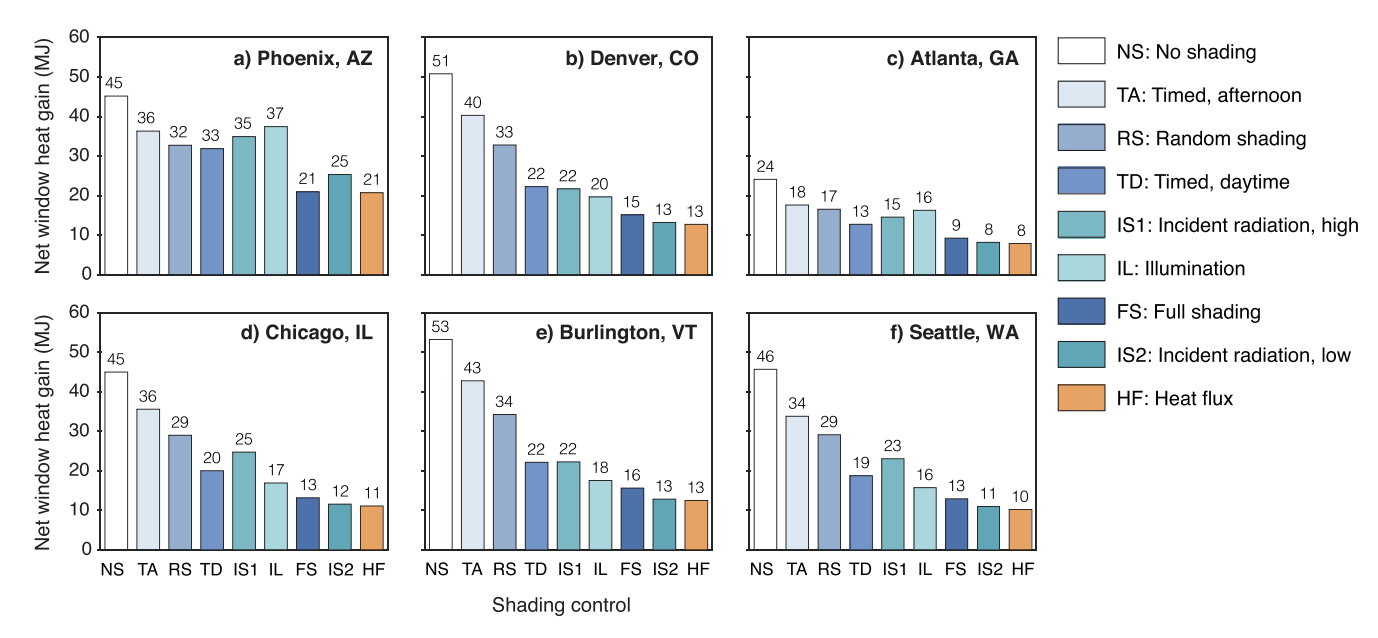


**Fig. 3.** Shading effectiveness under established and heat flux-based control strategies across climates. Net heat gain by total dwelling window area (5.1 m²; Table 2) over the days of July 16–18, inclusive, in the following cities and climate types: a) Phoenix, AZ (hot desert); b) Denver, CO (cold semi-arid); c) Atlanta, GA (humid subtropical); d) Chicago, IL (hot-summer humid continental); e) Burlington, VT (warm-summer humid continental); and f) Seattle, WA (Mediterranean). Control strategies, with noise-free sensed parameters: NS: no shading; TA: time-based afternoon shading (2p–8p); RS: randomly chosen shading operation; TD: time-based daytime shading (10a–4p); IS1: shading active above the incident solar radiation threshold of 250W/m²; IL: shading active above the illumination setpoint of 5000lux, at a position 20cm inside the window, and retracted below 500lux; FS: full (i.e., continuous) shading; IS2: shading active above the incident solar radiation threshold of 50W/m²; HF: shading active when window heat flux into the dwelling is positive (see also Table 3).

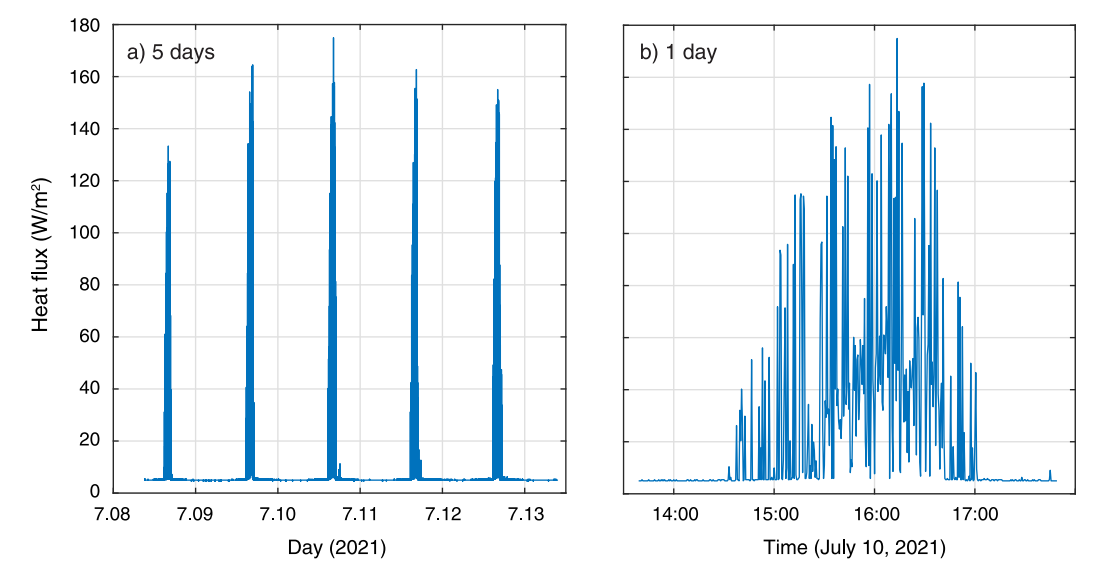


Fig. 4. Unprocessed heat flux signals showing characteristic noise. Heat flux measurements (W/m<sup>2</sup>) were recorded by a FluxTeq PHFS-01e thermopile heat flux sensor on the interior surface of a west-facing window at the University of Oregon a) during the period of July 8–13, 2021 and b) on July 10, 2021, expanded to show noise characteristics.

with periods of greater than one minute, by a factor of 8 or more (Fig. 5a). Autocorrelation within the same data was next analyzed using the MATLAB autocorr function, with time lags of 0 to 33.3 h at 30s intervals; this showed, similarly, that the only substantial repeating fluctuations in the heat flux measurements consisted of diurnal variations (Fig. 5b).

To reveal the distribution of deviations from true signals that constituted noise, we next collected heat flux readings at  $126\,\mathrm{ms}$  intervals over numerous  $2\,\mathrm{min}$  periods on multiple days. Heat flux values were effectively constant over each of these periods, with net changes of less than  $0.001\,\mathrm{W/m^2}$  in each case, allowing the associated noise to be extracted by subtracting the mean. Among

the resulting noise samples, mean values ranged from -0.12– $0.18 \text{W/m}^2$ , and standard deviations ranged from 25.8–37.1 W/  $\text{m}^2$ , consistent with values found in the July 8–13 dataset above. One of these samples ( $\sigma$ =28.1 W/ $\text{m}^2$ , with distribution shown in Fig. 6) was subsequently used to create realistic noise for application to simulated heat flux signals.

# 3.4. Effects of heat flux noise on shading performance

Given the noise characteristics above, we next examined the effects of a range of noise values on heat flux-controlled shading performance, expressed as the total dwelling net window heat gain

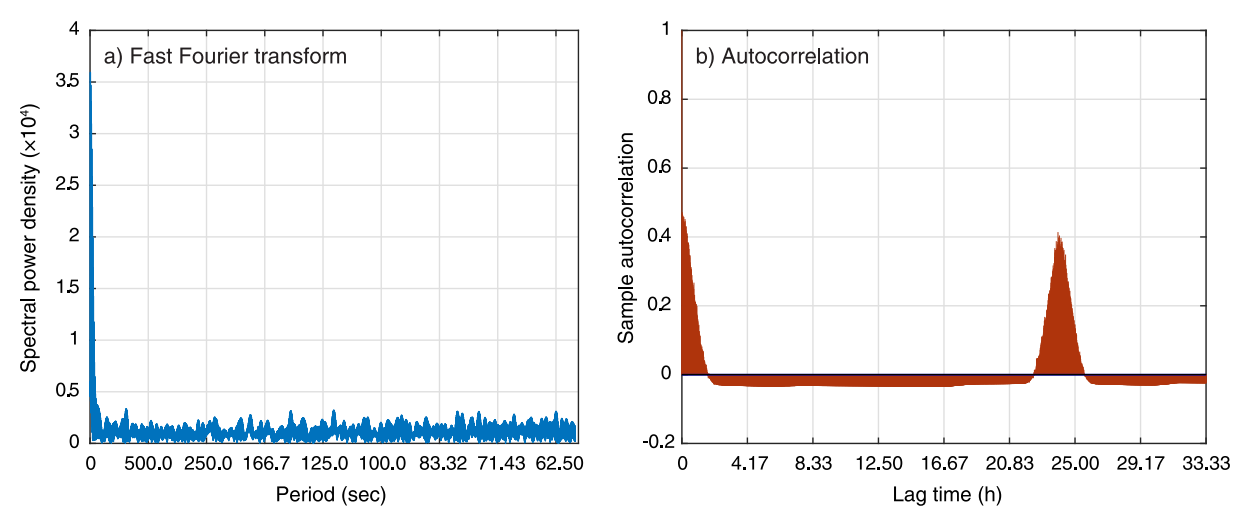


**Fig. 5.** Periodicity in heat flux signals. Heat flux measurements recorded by a FluxTeq PHFS-01e sensor on the interior surface of a west-facing window at the University of Oregon from July 8–12, 2021 (Fig. 4) were subjected to a) a fast Fourier transform, examining periods as short as one minute, and b) an autocorrelation analysis, examining time lags of 30 s from zero to 33.3 h.

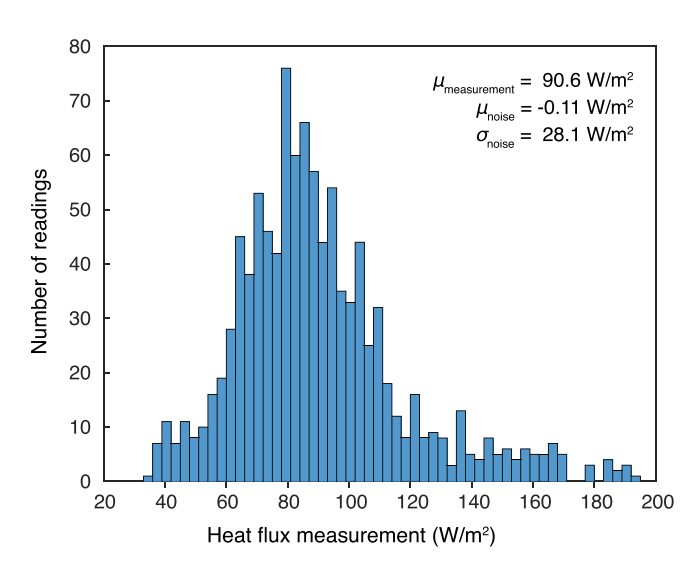


**Fig. 6.** Heat flux measurement distribution in the sample used to represent realistic noise. Values were recorded by FluxTeq PHFS-01e sensors on the interior surface of a west-facing window at the University of Oregon, at approx. 126 ms intervals over a 2 min period on July 19, 2021. Data are shown in bins of  $3W/m^2$ .

summed over July 16–18, inclusive, among the six climates. Window heat gain is shown both as a function of the standard deviation of the noise distribution (Fig. 7) and, in the Supplementary Information, as a function of the signal to noise ratio (Fig.S4); multiple iterations were conducted to show the consistency of the results.

In each climate, the cooling performance of shading controlled by synthetic heat flux signals that incorporated additive noise, with standard deviations of the noise ranging from 0–500 W/m² (see Section 2.3.2), declined as noise increased (Fig. 7a). Within the lower range of noise levels, characterized by standard deviations of 0–50 W/m², net window heat gain increased steeply with noise. At higher noise levels, however, in which  $\sigma > 200 \text{W/m²}$ , window heat gain increased more gradually with increasing noise, yielding only marginally higher values at standard deviations of 300, 400, and 500 W/m². At these levels, net window heat gain approached that observed with randomly-controlled shading, indicating that high noise levels virtually obscured the heat flux signals

and caused erratic shade actions throughout each day. This pattern was found across all cities examined, though net window heat gain values differed among locations. Shading performance, and declines in performance with increasing noise, were comparable among the climates of Denver, Chicago, Burlington, and Seattle (Figs. 7a.ii and iv-vi, respectively): while window heat gain reached 45-50MI in the absence of shading, shading controlled by noise-free heat flux signals reduced heat gain to 10-15MJ, rising to 25-30 MJ when signals were highly noisy. Windows with heat fluxcontrolled shading in Phoenix (Fig. 7a.i), the warmest city in the study, experienced the greatest net heat gain, ranging from a low value of 20 MJ with noise-free signals to 32 MJ at the highest noise level. In contrast, windows in Atlanta (Fig. 7a.iii), with a similar latitude to that of Phoenix, experienced the lowest net heat gain (7-15 MJ). These results reflected the lower typical direct solar radiation intensity in July in Atlanta compared to Phoenix (Table 1) as well as the lower latitude of Atlanta relative to the more northern cities, resulting in higher July sun angles and lower resulting transmission of direct solar radiation through vertical glazing.

An analogous investigation of the influence of multiplicative noise in heat flux signals on window shading performance revealed similar patterns. Again, across noise levels corresponding to  $\sigma$ =0– 10 (see Section 2.3.2), shading performance diminished as noise in heat flux signals increased (Fig. 7b). In contrast to signals with additive noise, signals with very low levels of multiplicative noise ( $\sigma$ =0–0.5) caused negligible increases in net window heat gain, independent of climate. Higher multiplicative noise levels  $(\sigma=0.5-2)$  caused steep increases in net window heat gain across all climates, analogous to the steep increases observed a the lowest ranges of additive noise: greater noise, however, caused only small additional increases in net window heat gain as shade actions approached random behavior, as observed among signals with additive noise. Shading in Denver, Chicago, Burlington, and Seattle (Fig. 7b.ii and iv-vi, respectively) again performed comparably, with window heat gain values of 10-15 MJ observed with noisefree heat flux control, rising to 25-32MJ at high noise levels. Shaded windows in Phoenix (Fig. 7b.i) again experienced the highest net heat gain observed, ranging from 20-35 MJ across noise levels, while those in Atlanta (Fig. 7b.iii) again showed the lowest.

Together, these results showed that noise affects the usability of heat flux signals for shading control consistently across climate types, and that shading performance declines markedly with

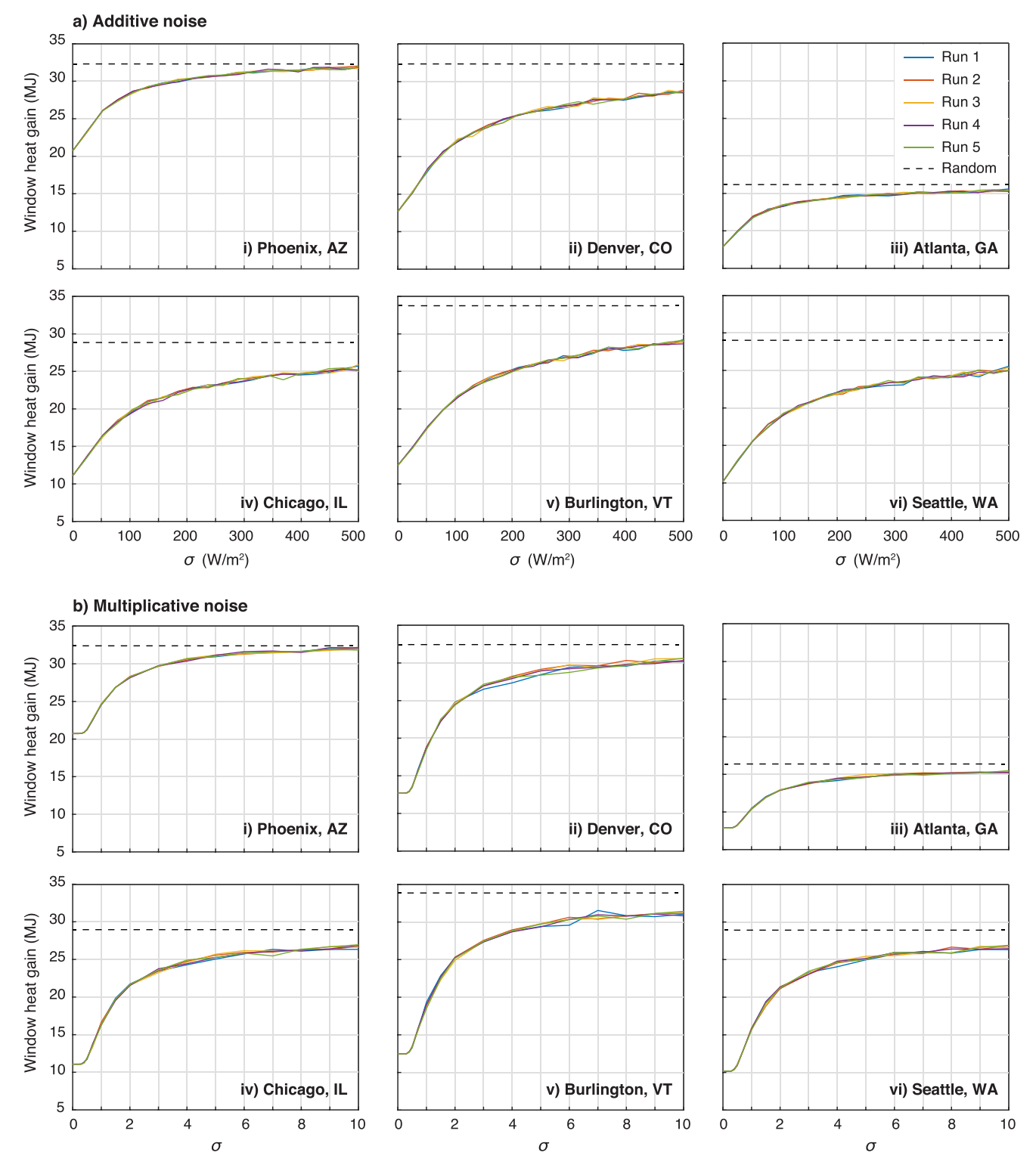
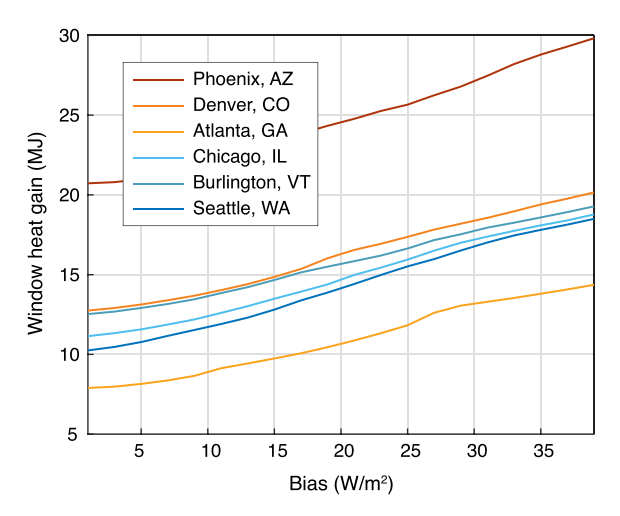


Fig. 7. Influence of signal noise on the cooling performance of heat flux-controlled shading. Net heat gain by total dwelling window area  $(5.1 \text{ m}^2; \text{Table 2})$  is shown for the period of July 16–18, inclusive. Insulated, edge-sealed shading was controlled by heat flux signals with a) synthetic additive noise  $(\sigma$ =0–500 W/m²) and b) synthetic multiplicative noise  $(\sigma$ =0–10; see Section 2.3.2), in i) Phoenix AZ; ii) Denver CO; iii) Atlanta GA; iv) Chicago IL; v) Burlington VT; and vi) Seattle WA. Shading was active when window heat flux into the dwelling exceeded 0W/m² and retracted otherwise; dotted lines show the performance of randomly operated shading (Table 3). Results are presented as functions of signal to noise ratios in the Supplementary Information, Fig.S4.

increasing noise at relatively low noise levels, depending on the additive and multiplicative characteristics of the noise. At higher levels, in contrast, the rate of performance decline with increasing noise slows, and window heat gain asymptotically approaches that allowed by randomly-controlled shading. Additionally, the transi-

tion between linear and asymptotic performance occurs at comparable noise levels across climates. These features indicate both that noise mitigation is essential for use of heat flux signals in shading control and that mitigation measures are likely to be comparably effective across climate types.



**Fig. 8.** Influence of signal bias on the cooling performance of heat flux-controlled shading. Net heat gain by total dwelling window area (5.1 m²; Table 2) is shown for the period of July 16–18, inclusive, in which insulating, edge-sealed shading was controlled by heat flux signals with negative biases of 0–40 W/m² under weather typical of 2004–2018 conditions [38] in Phoenix AZ (hot desert), Denver CO (cold semi-arid), Atlanta GA (humid subtropical), Chicago IL (hot-summer humid continental), Burlington VT (warm-summer humid continental), and Seattle WA (Mediterranean).

Investigation of signal bias also revealed a decline in shading performance with increasing offset of the heat flux signal from its true value (Fig. 8), allowing net window heat gain to increase at comparable rates in each climate studied. Though a uniform bias can be managed with effective calibration, the results of this analysis suggest that signal drift, i.e. increasing bias over long periods of time, could diminish the performance of heat flux controlled shading over the lifetime of a device. Measurements from the sensors used in this study suggest, however, that drift over periods of up to two years is likely to be negligible for the current purpose.

Next, to examine the effects of noise and bias in heat flux signals on shading actuation frequency, three contrasting levels of the additive and multiplicative synthetic noise models used above (Fig. 7) were injected into heat flux signals generated by Energy-Plus simulations using the Denver, CO weather file. These noisy signals were then used to control window shade opening and closing actions through co-simulation of EnergyPlus with MATLAB [43]. Without noise or bias, shades usually maintained the open or closed positions appropriate for cooling, but they opened and closed rapidly near each transition between heat loss and gain (Fig. 9a, b). This occurred because shading itself affected window heat flux, especially at values near zero: for example, positiveinward heat flux signals induced shade deployment; shade deployment lowered subsequent heat flux signals to zero or below; and the shade retracted in response, causing signals to return to positive values in the next timesteps. Not only could such rapid cycling annoy occupants, whether experienced as automatic oscillations or flickering messages requesting manual operation, but it could also compromise thermal performance by allowing unwanted window heat gain to occur when shades were counterproductively retracted, as illustrated by the positive heat flux spikes that occurred during shade oscillation in Fig. 9b.

Additive noise at low levels, characterized by a  $2 \, \text{W/m}^2$  standard deviation (Section 2.3.2), increased on/off shade cycling above that observed with noise-free signals by increasing the number of false-positive and false-negative heat flux values reported near transitions between outward and inward heat flux (Fig. 9c). At higher noise levels ( $\sigma$ =20 W/m²), numerous on/off cycles occurred in both morning and evening (Fig. 9d), and noise characterized by a 200 W/

m<sup>2</sup> standard deviation (Fig. 9e) caused nearly continuous on/off cycling throughout each day. Multiplicative noise caused less cycling than additive noise at low levels (Fig. 9f), as expected, because noise magnitudes were lowest near heat flux direction transitions when signals were also lowest. Oscillations increased at higher noise levels, as observed with additive noise, but remained distributed throughout each day rather than concentrated near morning and evening transition points because higher noise levels accompanied higher mid-day signal magnitudes (Fig. 9g). At the highest noise level, oscillations increased further, as expected, but maintained a similar distribution pattern (Fig. 9h). Because physically measured heat flux signals showed characteristics of both additive and multiplicative noise (e.g., Fig. 4b), resembling a blend of Figs.9d and 9g, this investigation of synthetic noise suggested that diminishing noise levels to those shown in Figs. 9c and 9f would beneficially constrain shade actions to the desired morning and evening transitions but would not necessarily diminish oscillation behavior to acceptable levels. Bias in heat flux signals also increased the number of shade control actions. A negative discrepancy of 5 W/m<sup>2</sup> between apparent and true heat flux values added several (<10) cycles to each morning and evening transition (compare Fig. 9a to 9i); an analogous bias of 10W/m<sup>2</sup> (Fig. 9j) approximately doubled this number; and a bias of 30W/m<sup>2</sup> (Fig. 9k) increased cycling substantially.

At each noise and bias level examined, rapid shade cycling occurred near the transition between inward and outward heat flux, continuing until the direction of net heat flux was unchanged by the shade position. While numerous approaches exist to dampen such oscillations when signals are clean, deadbands and nonzero heat flux thresholds were not sufficient to eliminate oscillations and maintain cooling performance with the current noisy signals, requiring investigation of noise mitigation measures.

# 3.5. Effectiveness of digital filters and persistence requirements

With the goal of reducing net window heat gain and unnecessary shading on/off cycling simultaneously, we next examined the effectiveness of digital filtering of noisy heat flux signals, signal persistence requirements, and combinations of the two. A recent investigation by Jung et al. [31] showed excellent performance by Savitzky-Golay filtering in reducing heat flux signal noise while maintaining the shape and height of peaks; here, however, we sought simpler filters to limit the computational requirements of future sensing and actuation devices. This investigation injected realistic noise (Section 2.3) into clean EnergyPlus-simulated window heat flux signals calculated from solar radiation values in the corresponding weather files; treated the signals as described in each corresponding section below; and reported the shading on/off actions directed by the resulting treated signals over three July days. Noise-free heat flux signals for windows without shading (Fig. 10a) illustrate the maximum window heat gain values possible in the current configuration, in the climate of Denver CO, while those for windows with continuous shading illustrate the minimum daytime values possible with the shading provided (Fig. 10b). Additionally, noisy heat flux signals and corresponding actions in the absence of filtering (Fig. 10c) illustrate the problematic on/off cycling. Imposition of a persistence requirement, necessitating a 40 min duration (Eqn. 5) of non-positive heat flux readings before activated shading could be retracted (but not affecting shade activation), eliminated the majority of on/off cycles despite the noisy signal (Fig. 10d); the value of 40 was found to be nearly optimal over the range of 5-75 one-minute timesteps under the current shading and dwelling configurations (Fig.S1). This intriguing result suggests that, even in the absence of further intervention, simple signal-persistence requirements can greatly improve the usability of noisy heat flux signals in shading control.

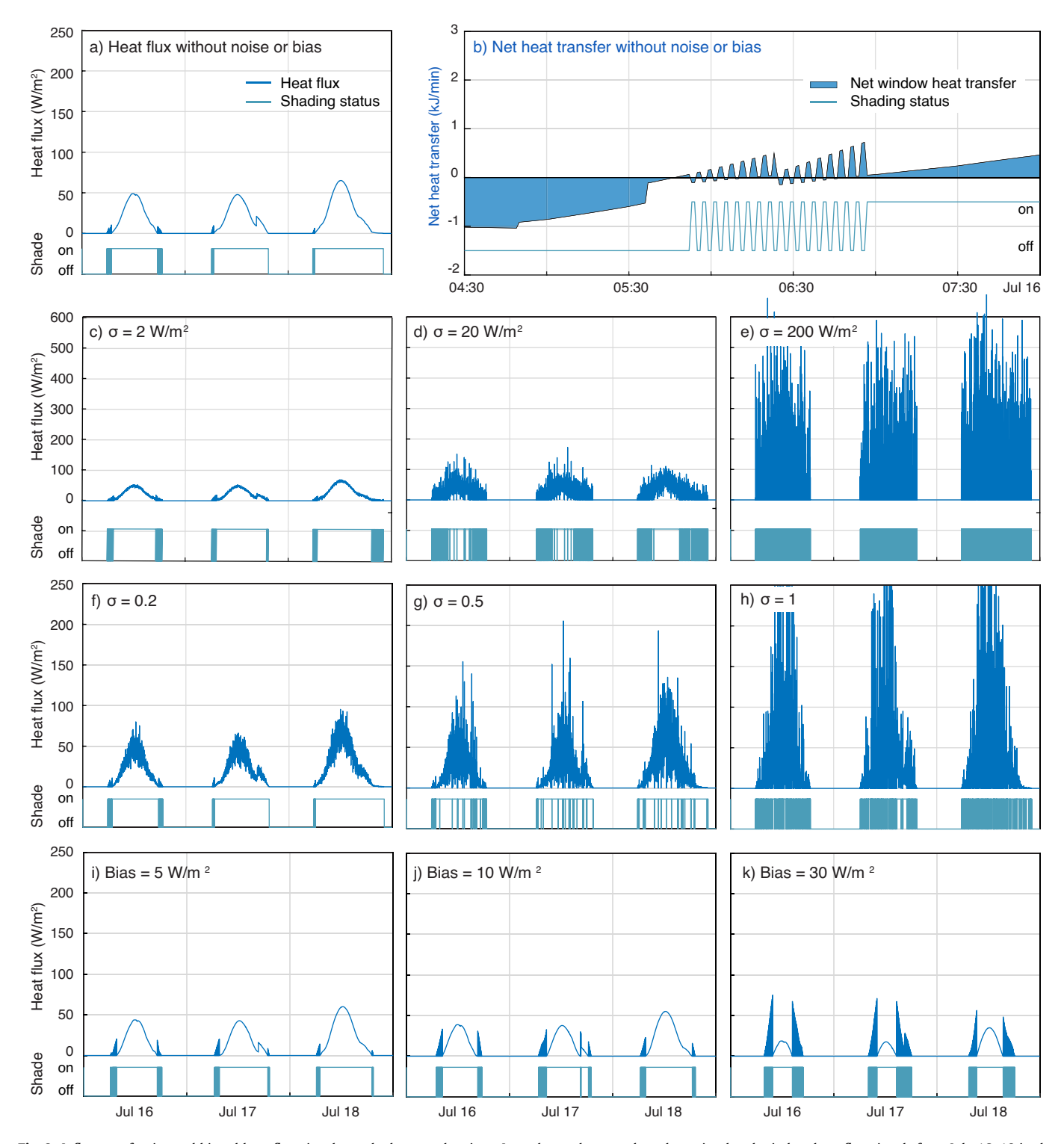


**Fig. 9.** Influence of noisy and biased heat flux signals on shade control actions. In each panel, upper data show simulated window heat flux signals from July 16–18 in the semi-arid climate of Denver, CO, with synthetic noise or bias, except for b) showing net heat transfer; lower data show corresponding on/off shading control actions for shading controlled by heat flux signals: a–b) without noise or bias, showing a) the signal and shading actions and b) expansion of the resulting window heat flux; c–e) with additive noise of  $\sigma$ =2, 20, and 200 W/m², respectively; f–h) with multiplicative noise of  $\sigma$ =0.2, 0.5, and 1, respectively (Section 2.3.2); and i–k) with bias levels of 5, 10, and 30 W/m², respectively. Shading was active during positive heat flux into the dwelling and retracted otherwise.

Endpoint moving average (EMA) filters, in which each heat flux value was replaced with the average of *N* previous measurements (Eqn. 3), were similarly effective (Fig. 10e); here, an interval of 20 1-min timesteps proved to be optimal (Fig. S1). This process produced a cleaner signal and greatly diminished the number of on/off cycles, although cycling was not reduced to the extent accom-

plished by the persistence requirement. Combining the EMA filter and the persistence requirement, however, eliminated all extraneous on/off cycling (Fig. 10f); it also diminished daytime window heat gain nearly to the level observed under continuous-shading conditions in Fig. 10b. An infinite impulse response (IIR) filter (Eqn. 4) was also highly effective, improving slightly upon the

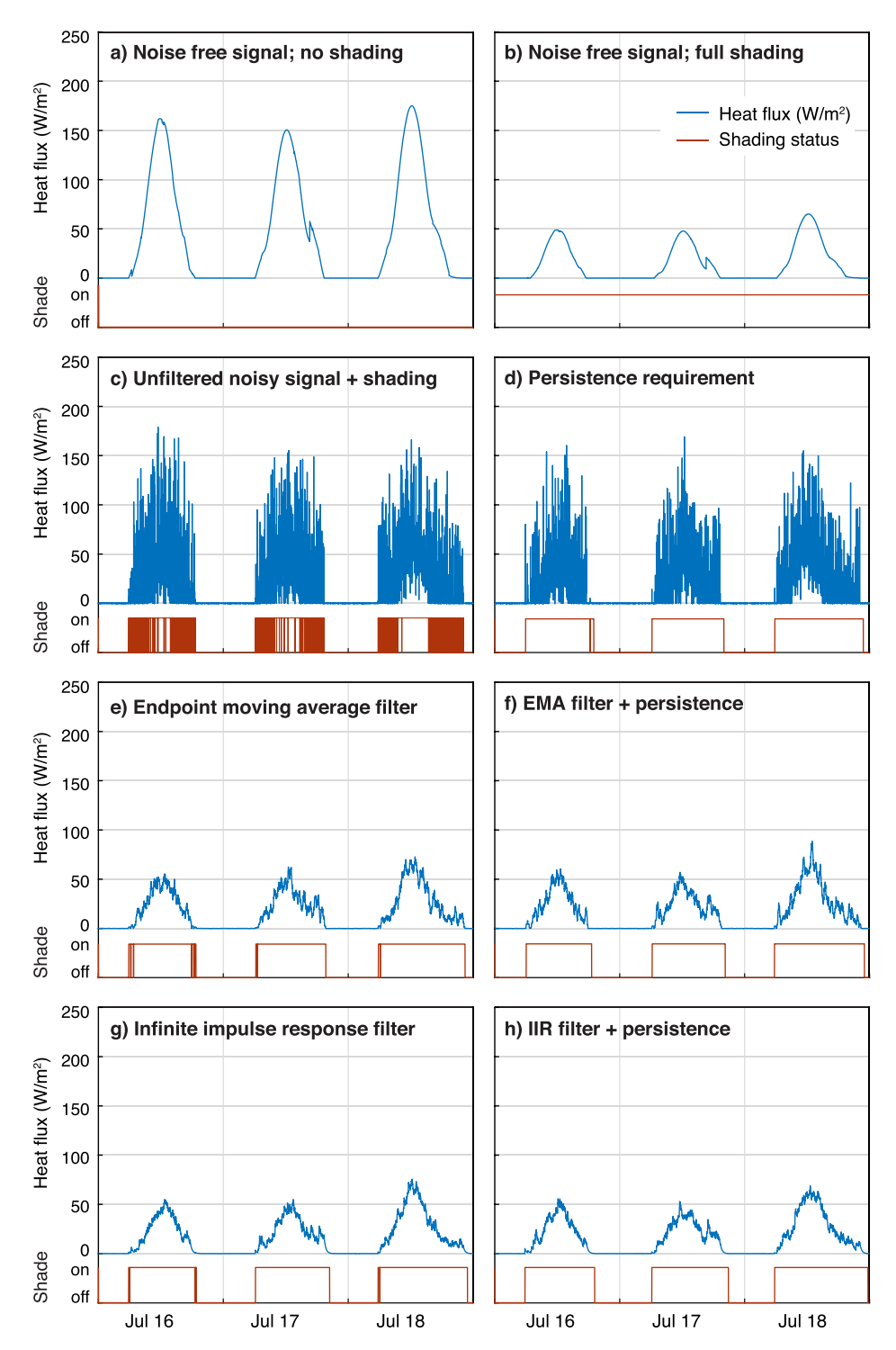


**Fig. 10.** Influence of heat flux signal processing on shade actuation frequency. In each panel, upper data show model-derived heat flux signals; lower data show corresponding shading on/off actions, with shading active when inward window heat flux exceeded  $0 \text{ W/m}^2$ . For reference, noise-free signals are shown a) without shading and b) with continuous shading. Realistic noise ( $\sigma$ =28.1 W/m²) was added (see Section 2.3) to evaluate signal processing and interpretation, showing results obtained by c) unfiltered noisy signals; d) a persistence requirement in which P = 40; e) an endpoint moving average (EMA) filter (N = 20); f) an EMA filter (N = 20) combined with the persistence requirement; g) an infinite impulse response (IIR) filter ( $\alpha$ =0.95); and h) an IIR filter ( $\alpha$ =0.95) with the persistence requirement. Simulations were conducted from July 16–18 using 2004–2018 weather data typical of Denver, CO.

EMA filter and reducing cycling almost entirely (Fig. 10g). In this case, an  $\alpha$  value of 0.95 was found to be nearly optimal (Fig. S1), removing fluctuations greater than 20 min in frequency. Additionally, combining the IIR filter with the 40 min persistence requirement eliminated all extraneous on/off cycling (Fig. 10h), as observed for the EMA filter above.

Ultimately, the effectiveness of filtered heat flux signals and persistence requirements in shading control depended on their abilities to reduce both net window heat gain and rapid on/off cycling consistently in varying climates. To investigate, we first compared configurations without shading and with random shade operation, as well as shading controlled by unfiltered heat flux sig-

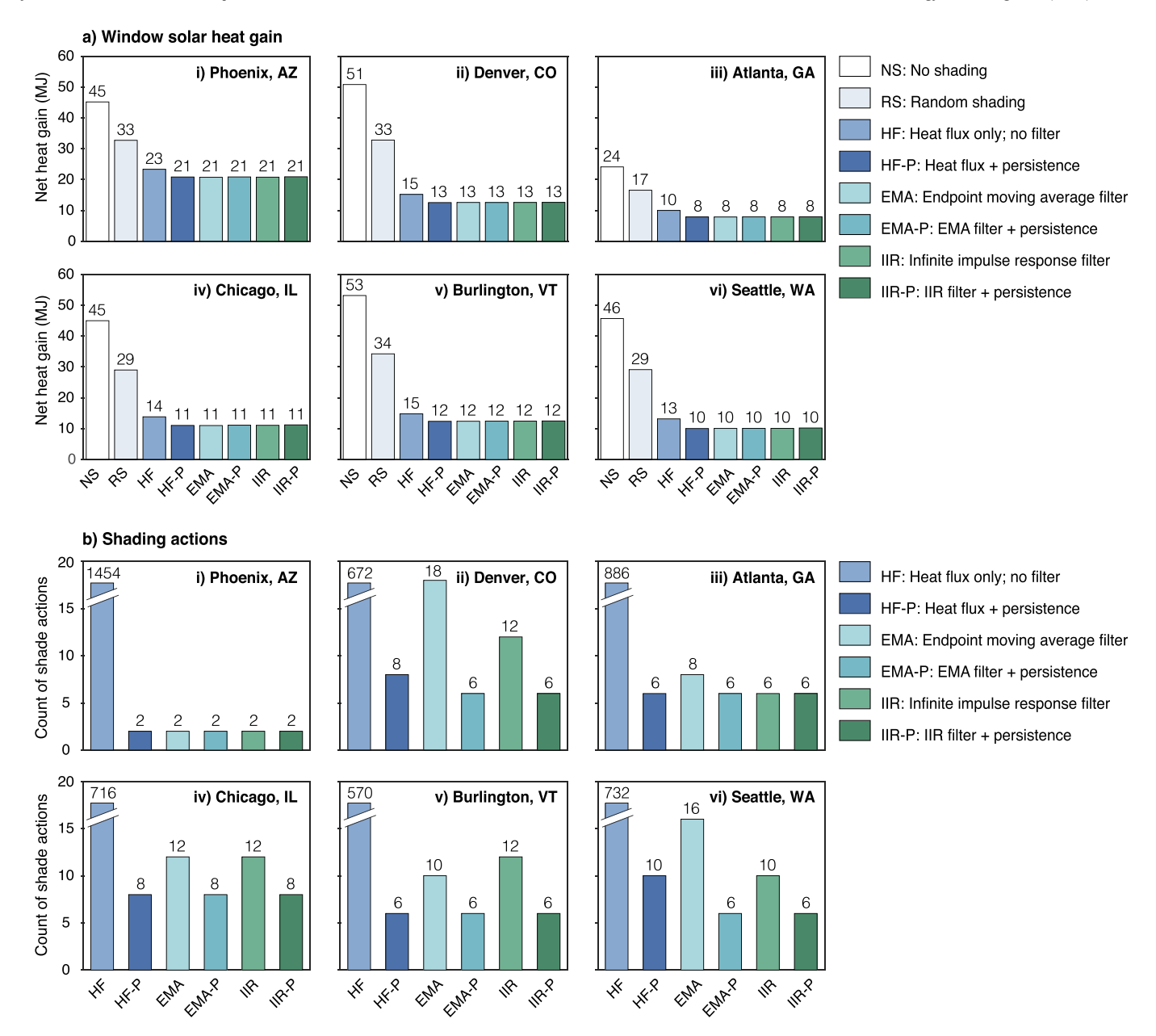


**Fig. 11.** Cooling performance of shading controlled by noise-mitigated heat flux signals across climates. a) Dwelling net window heat gain and b) shading on/off cycling frequency in i) Phoenix, AZ (hot desert); ii) Denver, CO (cold semi-arid); iii) Atlanta, GA (humid subtropical); iv) Chicago, IL (hot-summer humid continental); v) Burlington, VT (warm-summer humid continental); and vi) Seattle, WA (Mediterranean), using typical 2004–2018 weather data from July 16–18, inclusive (Table 1). Realistic noise (σ=28.1 W/m²) was injected into model-derived heat flux signals as in Fig. 10. Shading control strategies are designated NS: no shading; RS: random shading (Table 3); HF: shading during positive window heat flux into the dwelling; EMA: HF + endpoint moving average filter (N = 20); IIR: HF + infinite impulse response filter (σ=0.95); and P: including a persistence requirement (P = 40). A count of 6 shading actions indicates that one activation and one retraction occurred each day. Analogous results for signals with higher noise levels are shown in the Supplementary Information, Fig. S5.

nals, to filtered signals with and without persistence requirements across the six climates considered above: hot-desert (Phoenix AZ), cold semi-arid (Denver CO), humid subtropical (Atlanta GA), humid continental (Chicago IL and Burlington VT), and Mediterranean (Seattle WA) (Fig. 11a). Shades responding to heat flux signals that had been filtered with EMA and IIR filters, with and without persistence requirements, reduced window heat gains to the levels observed with shades controlled by clean heat flux signals in all cities (Fig. 3), showing that the filters and persistence requirements virtually eliminated the influence of noise on cooling performance. Persistence requirements alone achieved comparable window heat gain reductions.

Among the climates considered, windows in Phoenix and Atlanta (Figs.11a.i and 11a.iii) showed the least improvement, with reductions of 24 MJ and 16 MJ respectively, over the three-day period of July 16–18. This result reflected both code requirements for lower window solar heat gain coefficients in these climates, compared to those in cooler climates ([11]; Table 2), as well as the warmth of nighttime outdoor air and sky temperatures, diminishing the ability of unshaded windows to lose heat at night (see Fig. 2a, showing nighttime heat loss in Denver). Still, shading in these climates diminished net window heat gain by 54% and 60% of the unshaded totals, respectively. Shading in Denver and Burlington, in contrast, showed the greatest effectiveness, reducing

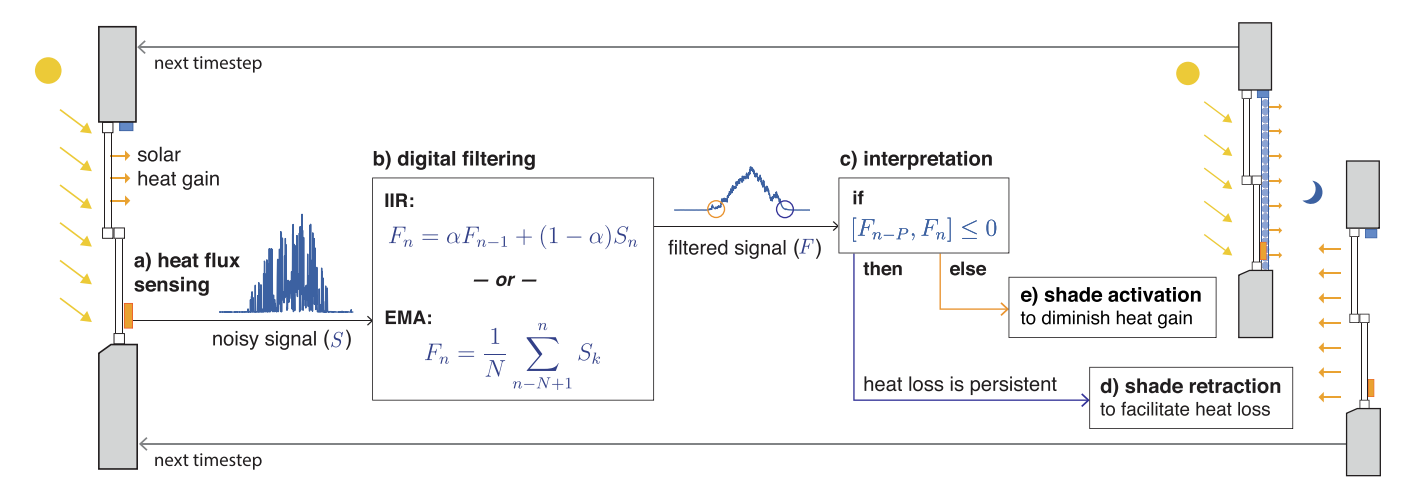


**Fig. 12.** Process overview. a) A heat flux sensor adhered to an interior window surface records a noisy signal, *S.* b) Digital filtering by either infinite impulse response (IIR) or endpoint moving average (EMA) filters reduce this noise, creating a filtered signal *F* that can be interpreted by *c*), the shading control algorithm. When cooling is desired, the detection of persistent heat loss directs the actuator to d) retract shading to diminish heat gain, while shading is otherwise e) activated to diminish heat gain. Symbols: *n*: current timestep; α: IIR coefficient; *N*: number of timesteps in the persistence interval.

window heat gain by 38 and 41 MJ (Figs.11a.ii and 11a.v), reflecting their higher window solar heat gain coefficients as well as cooler nighttime air and sky temperatures; these values amounted to 75% and 77% of the corresponding unshaded totals. Shading in Chicago and Seattle reduced window heat gain by intermediate values of 34 and 36 MJ, corresponding to 76% and 78% of the unshaded totals (Figs. 11a.iv and 11a.vi). Application of EMA and IIR filters and persistence requirements to considerably noisier signals, reflecting the levels shown in Figs.9e and 9h, allowed heat flux-controlled shading to achieve equal reductions in window heat gain (Fig. S5).

Together, these results showed that shading devices controlled by noisy heat flux signals treated with EMA or IIR filters, with and without persistence requirements, and with persistence requirements in the absence of filters, were virtually indistinguishable in their abilities to reduce window heat gain; additionally, they outperformed shading controlled by unprocessed heat flux signals as well as those controlled by established parameters (Fig. 3), acknowledging that setpoints for illumination and incident solar radiation were not optimized for the space, season, and climates studied here. Because of this comparability in cooling performance, the evaluation of heat flux signal treatment methods turned to their respective abilities to diminish erratic shade on/off cycling across the six climates (Fig. 11b).

In semi-arid Denver CO, humid-subtropical Atlanta GA, warmsummer humid continental Burlington VT, and Mediterranean Seattle WA (Fig. 11b.ii, iii, v, vi), EMA and IIR filtering of signals, with 40-min persistence requirements, reduced shading actions to one complete cycle each day, consisting of one activation in the morning to reduce daytime solar heat gain and one retraction in the evening to allow nighttime heat loss. Chicago IL (hotsummer humid continental) experienced one additional on/off cycle due to rain (Fig. 11b.iv), while in Phoenix, warm nighttime outdoor air and cooler interiors caused net heat flux to remain inward throughout much of the three-day period, causing shading to remain deployed for the majority of the time whether controlled by heat flux signals subject to filters, persistence requirements, or combinations of the two (Fig. 11b.i). Application of these filters and persistence requirements to signals with higher noise levels, represented by Figs.9e and 9h, showed equivalent results in all cities except Denver and Seattle; in each of these, one additional cycle was observed over the three-day July period (Fig. S5).

The striking result of this investigation is that two straightforward digital filters, with accompanying signal persistence requirements, each accomplished virtually complete elimination of erratic on/off cycling near heat flux direction transitions while maintaining excellent shading performance for cooling, as summarized in Fig. 12. This result indicates, further, that heat flux signals have additional potential for use in systems that integrate multiple parameters to meet composite goals addressing visual comfort and lighting energy use as well as cooling loads.

#### 4. Conclusions

This study investigates the feasibility of using direct measurements of window surface heat flux for the control of operable shading devices in passive cooling applications. Window heat flux is a promising metric for cooling-motivated shading control because it quantifies window heat gain directly, in contrast to the typical shading control parameters of illumination, glare indices, incident and transmitted solar radiation, indoor and outdoor air temperatures, and time of day. Additionally, its straightforward 0 W/m<sup>2</sup> setpoint, distinguishing inward from outward heat flux, has the potential to provide a universal threshold for actuation. Accordingly, shading controlled by clean heat flux signals showed the ability to reduce mid-summer window heat gain to equal or greater extents than shading controlled by established control parameters (Fig. 2), diminishing it by 54-78% in six contrasting climates (Fig. 3). The use of heat flux sensing in shading control has been limited, however, by issues of cost, physical fragility, high signal noise, and exclusion from standard shading control algorithms in building energy simulation tools. To our knowledge, only two studies have previously employed calculations of heat flux for shading or movable insulation control [44,49], and none have investigated the use of noisy heat flux data collected by physical sensors for such control.

The recent emergence of low-cost, durable heat flux sensors, however, addresses the problems of cost and fragility, inviting further exploration into the mitigation of sensor noise. Using inexpensive (\$50) FluxTeq, Inc. sensors and an Arduino apparatus (Fig. 1), we recorded heat flux at the surfaces of multiple double-glazed windows at the University of Oregon; characterized the noise in these signals; and estimated the effects of such noise on shading control through EnergyPlus simulations in multiple climates.

Among noise extracted from measurements collected on multiple days and times of day, means were consistently near zero, and standard deviations consistently ranged from approximately 25 to 40W/m². Application of representative field-derived noise to EnergyPlus-generated heat flux signals followed by shading control simulation, next confirmed that noisy heat flux signals are unsuitable for shading control because frequent over- and underestimations of true heat flux values lead to rapidly oscillating shade actions (Fig. 9).

Filtering of these noisy signals with either endpoint movingaverage (EMA) or infinite impulse response (IIR) filters reduced erratic shading control actions by more than 98%, however, as did the application of a requirement for continuous non-positive values over a period of 40 min before deployed shades could be retracted (Fig. 10). Combinations of filters and persistence requirements eliminated erratic actions entirely while reducing net window heat gain values to those observed with clean signals, using the transition between heat loss and heat gain as a consistent shading activation threshold, across six distinct climates (Fig. 11): ultimately, July net window heat gain was reduced by over 50% in the hot desert climate of Phoenix AZ and in the humid subtropical climate of Atlanta GA, while reductions of over 70% were found in semi-arid Denver CO, hot-summer continental Chicago IL, warm-summer continental Burlington VT, and Mediterranean Seattle WA.

These results present convincing evidence that heat flux sensing, with noise mitigation and signal persistence requirements, has excellent potential as an effective strategy for controlling window shading for cooling purposes (Fig. 12). With the emergence of low-cost sensors, it also has the potential for greater affordability than incident or transmitted solar radiation sensing. In applications that optimize shading operation to balance multiple objectives, including illumination, visual comfort, and/or views to the outdoors in addition to space cooling, heat flux sensing likewise has the potential to contribute a direct measure of window heat gain, allowing the universal setpoint of  $0 \text{W/m}^2$  to indicate the transition between window heat gain and loss and simplifying requirements for additional environmental information.

# Code and product availability

All MATLAB codes, recorded heat flux data, and EnergyPlus models are available upon request.

# **CRediT authorship contribution statement**

**Jackson Danis:** Conceptualization, Methodology, Data curation, Software, Validation, Formal analysis, Investigation, Visualization, Writing - original draft, Writing - review & editing. **Sandipan Mishra:** Conceptualization, Methodology, Writing - review & editing, Supervision, Funding acquisition. **Alexandra R. Rempel:** Conceptualization, Methodology, Investigation, Visualization, Resources, Writing - original draft, Writing - review & editing, Software, Funding acquisition, Project administration.

#### **Declaration of Competing Interest**

The authors declare that they have no known competing financial interests or personal relationships that could have appeared to influence the work reported in this paper.

## Acknowledgements

We gratefully acknowledge the contributions of Rowan Atherley and Philippa Bailey in building energy model construction, as well as the preliminary methodological development conducted by Julianna Chiaramonte, a recent graduate of Rensselaer Polytechnic Institute, and by Joseph Bostick of West Point Academy. We further acknowledge the facilitation of this project by Colin Meyer of Dartmouth College and the technical support of Chris Cirenza of FluxTeq LLC. This work was funded by the U.S. National Science Foundation through grant CBET-1804218, including two Research Experiences for Undergraduates supplements.

# Appendix A. Supplementary data

Supplementary data associated with this article can be found, in the online version, at <a href="https://doi.org/10.1016/j.enbuild.2022.111950">https://doi.org/10.1016/j.enbuild.2022.111950</a>.

#### References

- International Energy Agency, The Future of Cooling: Technical Report, Paris, FR (2018). https://www.iea.org/reports/the-future-of-cooling.
- [2] O. Lucon, D. Ürge-Vorsatz, A. Zain Ahmed, H. Akbari, P. Bertoldi, L. Cabeza, N. Eyre, A. Gadgil, L. Harvey, Y. Jiang, E. Liphoto, et al., Climate Change 2014: Mitigation of Climate Change: Contribution of Working Group III to the Fifth Assessment Report of the Intergovernmental Panel on Climate Change, Cambridge University Press, 2014, Ch. 9: Buildings..
- [3] Lawrence Livermore National Laboratory, Energy Flow Charts: 2020, Livermore, CA (2020). https://flowcharts.llnl.gov/content/assets/docs/ 2020\_United-States\_Energy.pdf..
- [4] U.S. Energy Information Administration, Annual Energy Outlook: Tables A4. Residential Sector Key Indicators and Consumption and A19. Energy-Related Carbon Dioxide Emissions by End-Use, U.S. Department of Energy, Washington D.C. (2021). https://www.eia.gov/outlooks/aeo/.
- [5] I. Oropeza-Peréz, P.A. Østergaard, Active and passive cooling methods for dwellings: A review, Renewable and Sustainable Energy Reviews 82 (2018) 531–544.
- [6] D.H. Li, J.C. Lam, Solar heat gain factors and the implications to building designs in subtropical regions, Energy and Buildings 32 (1) (2000) 47–55.
- [7] A. O'Donovan, M.D. Murphy, P.D. O'Sullivan, Passive control strategies for cooling a non-residential nearly zero energy office: Simulated comfort resilience now and in the future, Energy and Buildings 231 (2021) 110607.
- [8] J.-W. Lee, H.-J. Jung, J.-Y. Park, J. Lee, Y. Yoon, Optimization of building window system in asian regions by analyzing solar heat gain and daylighting elements, Renewable energy 50 (2013) 522–531.
- [9] E. Cuce, S.B. Riffat, A state-of-the-art review on innovative glazing technologies, Renewable and sustainable energy reviews 41 (2015) 695–714.
- [10] A. Tzempelikos, A.K. Athienitis, The impact of shading design and control on building cooling and lighting demand, Solar Energy 81 (3) (2007) 369–382.
- [11] International Code Council, International Energy Conservation Code (IECC), Ch. 4 [RE]: Residential Energy Efficiency, Washington D.C. (2018). https://codes.iccsafe.org/content/iecc2018/chapter-4-re-residential-energy-efficiency..
- [12] A.R. Rempel, A.W. Rempel, S. McComas, S. Duffey, C. Enright, S. Mishra, Magnitude and distribution of the untapped solar space-heating resource in U. S. climates, Renewable and Sustainable Energy Reviews 151 (2021) 111599.
- [13] D.K. Bhamare, M.K. Rathod, J. Banerjee, Passive cooling techniques for building and their applicability in different climatic zones—The state of art, Energy and Buildings 198 (2019) 467–490.
- [14] J. Cho, C. Yoo, Y. Kim, Viability of exterior shading devices for high-rise residential buildings: Case study for cooling energy saving and economic feasibility analysis, Energy and Buildings 82 (2014) 771–785.
- [15] A. Atzeri, F. Cappelletti, A. Gasparella, Internal versus external shading devices performance in office buildings, Energy Procedia 45 (2014) 463–472.
- [16] A.R. Rempel, S.J. Remington, Optimization of passive cooling control thresholds with GenOpt and EnergyPlus, in: Proceedings of the Symposium on Simulation for Architecture & Urban Design, 2015, pp. 103–110, Alexandria, VA..
- [17] Y.K. Yi, A.M. Malkawi, Thermal efficiency of the window shade, in: Proceedings of 11th International IBPSA Building Simulation Conference, Glasgow, UK, 2009, pp. 1693–1698..
- [18] Y. Tan, J. Peng, D.C. Curcija, R. Hart, J.C. Jonsson, S. Selkowitz, Parametric study of the impact of window attachments on air conditioning energy consumption, Solar Energy 202 (2020) 136–143.
- [19] S. Firlag, M. Yazdanian, C. Curcija, C. Kohler, S. Vidanovic, R. Hart, S. Czarnecki, Control algorithms for dynamic windows for residential buildings, Energy and Buildings 109 (2015) 157–173.
- [20] P.C. da Silva, V. Leal, M. Andersen, Influence of shading control patterns on the energy assessment of office spaces, Energy and Buildings 50 (2012) 35–48.
- [21] A. Tzempelikos, H. Shen, Comparative control strategies for roller shades with respect to daylighting and energy performance, Building and Environment 67 (2013) 179–192.
- [22] A.M. Atzeri, A. Gasparella, F. Cappelletti, A. Tzempelikos, Comfort and energy performance analysis of different glazing systems coupled with three shading control strategies, Science and Technology for the Built Environment 24 (5) (2018) 545–558.

- [23] A. Tabadkani, A. Roetzel, H.X. Li, A. Tsangrassoulis, A review of automatic control strategies based on simulations for adaptive facades, Building and Environment 175 (2020) 106801.
- [24] C. Carletti, F. Sciurpi, L. Pierangioli, F. Asdrubali, A.L. Pisello, F. Bianchi, S. Sambuco, C. Guattari, Thermal and lighting effects of an external venetian blind: Experimental analysis in a full scale test room, Building and Environment 106 (2016) 45–56.
- [25] A. Al Touma, D. Ouahrani, Shading and day-lighting controls energy savings in offices with fully-glazed façades in hot climates, Energy and Buildings 151 (2017) 263–274.
- [26] S. Grynning, B. Time, B. Matusiak, Solar shading control strategies in cold climates-heating, cooling demand and daylight availability in office spaces, Solar Energy 107 (2014) 182–194.
- [27] G. Van Moeseke, I. Bruyère, A. De Herde, Impact of control rules on the efficiency of shading devices and free cooling for office buildings, Building and Environment 42 (2) (2007) 784–793.
- [28] J. Hu, P. Karava, Model predictive control strategies for buildings with mixed-mode cooling, Building and Environment 71 (2014) 233–244.
- [29] A.R. Rempel, S. Lim, Numerical optimization of integrated passive heating and cooling systems yields simple protocols for building energy decarbonization, Science and Technology for the Built Environment 25 (9) (2019) 1226–1236.
- [30] A. Mavrogianni, M. Davies, J. Taylor, Z. Chalabi, P. Biddulph, E. Oikonomou, P. Das, B. Jones, The impact of occupancy patterns, occupant-controlled ventilation and shading on indoor overheating risk in domestic environments, Building and Environment 78 (2014) 183–198.
- [31] W. Jung, F. Jazizadeh, T.E. Diller, Heat flux sensing for machine-learning-based personal thermal comfort modeling, Sensors 19 (17) (2019) 3691.
- [32] D.L. Marinoski, S. Güths, F.O. Pereira, R. Lamberts, Improvement of a measurement system for solar heat gain through fenestrations, Energy and Buildings 39 (4) (2007) 478–487.
- [33] Z. Gao, E.S. Russell, J.E. Missik, M. Huang, X. Chen, C.E. Strickland, R. Clayton, E. Arntzen, Y. Ma, H. Liu, A novel approach to evaluate soil heat flux calculation: An analytical review of nine methods, Journal of Geophysical Research: Atmospheres 122 (13) (2017) 6934–6949.
- [34] P. Biddulph, V. Gori, C.A. Elwell, C. Scott, C. Rye, R. Lowe, T. Oreszczyn, Inferring the thermal resistance and effective thermal mass of a wall using frequent temperature and heat flux measurements, Energy and Buildings 78 (2014) 10– 16.
- [35] T.E. Kuhn, Calorimetric determination of the solar heat gain coefficient g with steady-state laboratory measurements, Energy and Buildings 84 (2014) 388– 402
- [36] A.R. Rempel, A.W. Rempel, K.V. Cashman, K.N. Gates, C.J. Page, B. Shaw, Interpretation of passive solar field data with EnergyPlus models: Unconventional wisdom from four sunspaces in Eugene, Oregon, Building and Environment 60 (2013) 158–172.

- [37] U.S. Department of Energy, EnergyPlus Version 9.2.0, Building Technologies Office, Office of Energy Efficiency and Renewable Energy, Washington D.C. (2019). https://energyplus.net.
- [38] L.K. Lawrie, D.B. Crawley, Development of Global Typical Meteorological Years (TMYx), 2004-2018 (2019). http://climate.onebuilding.org.
- [39] Lawrence Berkeley National Laboratory, WINDOW 7.7, Building Technologies & Urban Systems: Windows & Daylighting, Berkeley CA (2019). https://windows.lbl.gov/tools/window/software-download.
- [40] Big Ladder Software, Euclid v0.9.4.2: An open-source geometry editor for SketchUp, Denver, CO (2017). https://bigladdersoftware.com/projects/euclid/.
- [41] M. Kottek, J. Grieser, C. Beck, B. Rudolf, F. Rubel, World map of the Köppen-Geiger climate classification updated, Meteorologische Zeitschrift 15 (3) (2016) 259–263.
- [42] F. Rubel, M. Kottek, Observed and projected climate shifts 1901–2100 depicted by world maps of the Köppen-Geiger climate classification, Meteorologische Zeitschrift 19 (2) (2010) 135.
- [43] J. Dostal, EnergyPlus Co-simulation Toolbox, v1.2.3.1. (2021). www.mathworks.com/matlabcentral/fileexchange/69074-energyplus-co-simulation-toolbox..
- [44] M. Liu, K.B. Wittchen, P.K. Heiselberg, Control strategies for intelligent glazed façade and their influence on energy and comfort performance of office buildings in Denmark, Applied Energy 145 (2015) 43–51.
- [45] J.B. Johnson, Thermal agitation of electricity in conductors, Physical Review 32 (1928) 97–109, https://doi.org/10.1103/PhysRev.32.97. https://link.aps. org/doi/10.1103/PhysRev.32.97.
- [46] H. Nyquist, Thermal agitation of electric charge in conductors, Physical Review 32 (1928) 110–113, https://doi.org/10.1103/PhysRev.32.110. https://link.aps. org/doi/10.1103/PhysRev.32.110.
- [47] M. Liu, P.K. Heiselberg, Y.I. Antonov, F.S. Mikkelsen, Parametric analysis on the heat transfer, daylight and thermal comfort for a sustainable roof window with triple glazing and external shutter, Energy and Buildings 183 (2019) 209– 221.
- [48] S. Grynning, A. Gustavsen, B. Time, B.P. Jelle, Windows in the buildings of tomorrow: Energy losers or energy gainers?, Energy and buildings 61 (2013) 185–192
- [49] D. Bastien, V. Dermardiros, A.K. Athienitis, Development of a new control strategy for improving the operation of multiple shades in a solarium, Solar Energy 122 (2015) 277–292.
- [50] A.R. Rempel, A.W. Rempel, K.R. Gates, B. Shaw, Climate-responsive thermal mass design for Pacific Northwest sunspaces, Renewable Energy 85 (2016) 981-993
- [51] Arduino, Reference: analogRead (2021). https://www.arduino.cc/reference/en/ language/functions/analog-io/analogread/..